Assessment of using liquidity index for the approximation of undrained shear strength of clay tills in Scania

Dagnija Andreasson

Dissertations in Geology at Lund University,
Master's thesis, no 550
(45 hp/ECTS credits)

Department of Geology
Lund University
2018

Assessment of using liquidity index for the approximation of undrained shear strength of clay tills in Scania

Master's thesis

Dagnija Andreasson

Department of Geology
Lund University
2018

Abbrevations and Symbols

$(q_t - \sigma_{v0})$ – net tip resistance (kPa)

CPT – cone penetration test

c_u – undrained shear strength (kPa)

c_{uCPT} – undrained shear strength from the Cone Penetration Test (kPa)

c_{uVST} – undrained shear strength from the Vane Shear Test (kPa)

c_v – undrained vane shear strength (kPa)

e – a mathematical constant of 2.71828

e_0 – void ratio (%)

f_s – sleeve friction (kPa)

g – standard gravity (9.81 m/s^2)

I_L – liquidity index

I_P – plasticity index (%)

l_c – clay content (%)

M' – a constant of $0{,}4096 \cdot 10^{-3}$ (m^3)

m – bulk mass (kg)

M – factor for estimating the liquid limit

m_s – mass of a dry sample

m_w – mass of water

N – factor for estimating the liquid limit

N_{ke} – empirical cone factor

N_{kt} – cone factor

P_a – a peak torque (Nm)

q_c – cone resistance (kPa)

q_t – total cone resistance (kPa)

R^2 – coefficient of determination

R_f – friction ratio (kPa)

u – pore pressure (kPa)

V– bulk volume (m^3)

VST – vane shear test

w – natural water content

w_L – liquid limit (%)

w_P – plastic limit (%)

γ – unit weight (kN/m^3)

μ – Bjerrum's correction factor

ρ – bulk density (kg/m^3)

σ_{v0} – effective vertical stress (kPa)

Contents

Cover Picture: A drill rig, Helsingborg, Sweden. Photo by the author, 2018

Assessment of using liquidity index for the approximation of undrained shear strength of clay tills in Scania

Dagnija Andreasson

Andreasson, D., 2018: Assessment of using liquidity index for the approximation of undrained shear strength of clay tills in Scania *Dissertations in Geology at Lund University*, *No. 900, 41pp. 45 hp (45 ECTS credits).*

Abstract: Undrained shear strength is a crucial parameter of the clay-rich sediments commonly used in the design process of geotechnical structures and is determined by several tests. As a considerable part of these tests are cost- and time consuming, it is of interest to investigate the potential relationship with shear strength (c_u) with alternative, easily measurable parameters, such as liquidity index (I_L). In this study, several field and laboratory methods were applied to collect samples, analyse physical properties, and determine undrained shear strength of three clay tills of Stångby and Simrishamn in the province of Scania in southern Sweden. In total, 23 disturbed samplings, 13 cone penetration tests (CPT), and 11 vane shear tests (VST) were performed. The natural water content and liquid and plastic limits were established from all disturbed samples and undrained shear strength was determined from CPT and VST. The results show that the liquidity index varies between -0.10 and 0.34 at Stångby and between -0.35 and 0.23 at Simrishamn. The undrained shear strength varies between 57 and 256 kPa at Stångby and between 179 and 763 kPa at Simrishamn. Only a partial relationship between the liquidity index and undrained shear strength was found in this study. The study shows that the wide range of the consistency of clay-rich sediments is crucial for the correlation between I_L and c_u, which was demonstrated by the relation being found only at Simrishamn.

Keywords: clay till, undrained shear strength, liquidity index, CPT.

Supervisor(s): Dan Hammarlund, Erika Tudisco

Subject: Quaternary Geology

Dagnija Andreasson, Department of Geology, Lund University, Sölvegatan 12, SE-223 62 Lund, Sweden. E-mail: dagnija.andreasson@gmail.com

Bedömning av att använda flytindex för att uppskatta den odränerade skjuvhållfastheten av lermorän i Skåne.

Dagnija Andreasson

Andreasson, D., 2018: Assessment of using liquidity index for the approximation of undrained shear strength of clay tills in Scania. *Examensarbeten i geologi vid Lunds universitet*, *Nr. 900, 41sid. 45 hp.*

Sammanfattning: Den odränerade skjuvhållfastheten är en viktig geoteknisk parameter som man behöver ha en god uppfattning om i samband med byggnation på lerrika jordarter. Då flertalet av de vanligen tillämpade undersökningsmetoderna är väldigt tidskrävande och kostsamma, finns det ett stort intresse för att undersöka hur alternativa och samtidigt mer enkelt mätbara parametrar, så som flytindex (I_L), förhåller sig till skjuvhållfastheten (c_u). I denna studie användes flera olika typer av laboratorietester och fältmetoder för att analysera fysikaliska egenskaper hos tre olika moränleror från Stångby och Simrishamn och därmed bestämma den odränerade skjuvhållfastheten hos dessa. Totalt togs 23 störda prover och på samma djup utfördes 13 spetstrycksonderingar (CPT) och 11 vingförsök (VST). Den naturliga vattenkvoten, flytgränsen och plasticitetsgränsen fastställdes på alla störda prover medan den odränerade skjuvhållfastheten bestämdes med hjälp av CPT och VST. Resultaten visar att flytindex varierar mellan -0.10 och 0.34 i Stångby och mellan -0.35 och 0.23 i Simrishamn. Den odränerade skjuvhållfastheten varierar mellan 57 och 256 kPa i Stångby och mellan 179 och 763 kPa i Simrishamn. Endast en partiell relation kunde fastslås mellan flytindex och odränerad skjuvhållfasthet, och tydligast samband kunde påvisas på proverna från Simrishamn. Studien visar att det krävs analys av en stor mängd prover med mycket stor skillnad i konsistens för att fastslå sambandet mellan flytindex och odränerad skjuvhållfasthet.

Nyckelord: lermorän, odränerad skjuvhållfasthet, flytindex, CPT.

Handledare: Dan Hammarlund, Erika Tudisco

Ämnesinriktning: Kvartärgeologi

Dagnija Andreasson, Geologiska institutionen, Lunds Universitet, Sölvegatan 12, 223 62 Lund, Sverige. E-post: dagnija.andreasson@gmail.com

1 Introduction

Building on clay-rich sediments can be challenging and includes several geotechnical issues. They have a complex interaction between clay minerals and water, which in turn provides low bearing and strength capacity. As the physicochemical interaction between clay particles, the water that fills the voids between the particles and the ions in the water affect the mechanical behaviour of clays, high clay mineral content in the soil contributes to clay minerals being more "active" as a result, such deposits are highly compressible, very plastic, have a low permeability and are subjected to shrinkage and swell (Mitchell and Soga, 2005). Water is strongly connected to clay particle surfaces, which results in plasticity.

In 1911, the Swedish agriculturist Albert Atterberg described two qualitative (liquid and plastic) limits based on the varying water content of clay. These limits are used for identification, characterization and classification of clay-rich sediments. Plasticity index (I_P) is the difference between liquid (w_L) and plastic (w_P) limits and is the range of water content at which clay-rich sediments display plastic properties, while the liquidity index (I_L) describes the relative consistency of the clay-rich sediments. After Karl von Terzaghi (1925) discovered the potential of the Atterberg limits in soil mechanics, many further studies were performed to establish relationships between various mechanical properties of clayey sediments, such as compression modulus and shear strength, and liquidity and plasticity indices. While there have been many studies carried out worldwide to establish the correlation between liquidity index and undrained shear strength (c_u), such investigations are not common in Sweden. Larsson (2008) and Vardanega and Haigh (2014) also write that the Atterberg limits give an introductory assessment of mechanical properties of soils. Interestingly, the plasticity index also gives a preliminary insight into the potential geotechnical issues since the clay content is quantitatively estimated by the plasticity index (Duncan et al., 2014). Therefore, the higher the index, the more clay in the soil.

Geotechnical investigations are very important since they provide significant information about various physical and mechanical soil properties which affect the design of upcoming constructions. This study investigates the relationship between the liquidity index and undrained shear strength. Undrained shear strength of clay-rich sediments is not a characteristic property of the material, but is dependent on the water content (w). Thus, it is suggested to correlate to a state-dependent index parameter, the liquidity index (Knappett and Craig, 2012). Undrained shear strength is defined as an internal resistance to failure per unit area of a material and is commonly used to analyse soil stability and lateral pressure on geotechnical structures. In clayey sediments, it is the undrained shear strength that controls the bearing capacity. There are several approaches to determine undrained shear strength. It is common that undrained shear strength is derived from cone penetration tests (CPT) and used in further calculations, as the direct shear test methods, such as vane shear test (VST), are less cost- and time-effective. Thus, it is of interest to test the potential relationship with shear strength obtained using different methods by applying alternative, easily measurable parameters such as liquidity index. In this study, indirect empirical equations are considered using the CPT and direct in-situ VST methods.

This master's thesis was developed in collaboration with the consultancy company Tyréns, and after the evaluation of Quaternary deposit maps, it was determined to take part in fieldwork at two sites: Stångby and Simrishamn. Sampling at both sites was performed during October and November 2017. As a fieldwork plan was followed, it largely determined the location of investigation points. Results from previous studies and proposed shear strength estimations from liquidity/plasticity indices are discussed in this thesis.

To carry out this thesis, a literature study of clayey sediments in the province of Scania was conducted. The aim of this study, which is based on a literature review complemented by selected field and laboratory analyses, is to evaluate the relationship between liquidity index and undrained shear strength to assess the possibility of using liquidity index as a means of estimating the undrained shear strength of clay tills in Scania.

Different limitations may arise when clay till is being analysed. Firstly, a clay till is inhomogeneous and generally includes large clasts as well as layers of coarse-grained sorted material. Thus, large clasts might influence or even interrupt the disturbed sampling. Secondly, not only the sampling is affected by clay till inhomogeneity, but also other in-situ testing methods. CPT is applicable to soft sediments and if the clay till contains coarse sand or gravel at the investigation point, the risk that the CPT will be interrupted is high. VST is another method that is sensitive to the presence of coarse material, since it might give higher undrained shear strength values.

At the Stångby and Simrishamn sites clay till was exposed at the surface. The initial observation of disturbed samples showed that the clay till at Stångby had enough clay to implement VST. In contrast, the clay till at Simrishamn was sandy, and so only CPT was carried out there. Clay content and grain size variations affect not only the choice of in-situ methods but also might have impacts on the results in laboratory tests.

2 Theoretical background

2.1 Clay till and its properties

2.1.1 Liquid and plastic limits

At the initial stage, the natural water content (w) of each sample is determined and calculated:

$$w = \frac{m_w}{m_s}\ (\%)$$

where m_w is the mass of water and m_s is the mass of a dry sediment sample (Swedish Standards Institute, 2008)

The water content at which a physical state of clayey sediments or their consistency changes from liquid to plastic and from plastic to brittle are defined as the liquid limit (w_L) and plastic limit (w_P), respectively (Fig. 2.1).

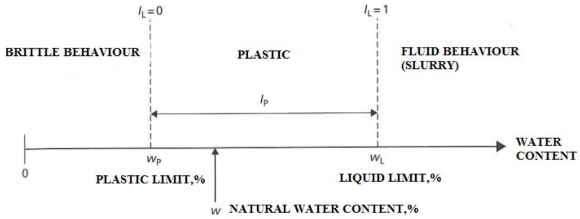

Figure 2.1. Atterberg limits (modified from Knappett and Craig, 2012).

The liquid limit (w_L) is determined by the fall cone method and calculated in the following way:

$$w_L = M \cdot w + N\ (\%)$$

where *w* is the water content of the sediment sample and *M* and *N* values are derived from appendix A (Larsson, 2008).

Named in honour of Albert Atterberg, this method is widely used due to its accessibility and simplicity for evaluation of consistency of clayey sediments.

Lastly, the plastic limit is determined as the lowest water content of the sediment sample at which the consistency changes from plastic to brittle.

2.1.2 Plasticity and liquidity indices

The plasticity index is the water content range in the clay-rich sediment sample at which it displays plastic properties, and it is defined as the difference between liquid and plastic limits (Venkatramaiah, 2006):

$$I_P = w_L - w_P\ (\%)$$

The greater this difference is, the more plastic the sediments are (Murthy, 2002).

The liquidity index describes the moisture level in the clay-rich sediments in the field and thus determines the plastic range of the sediments.

$$I_L = \frac{(w - w_P)}{I_P}$$

If the liquidity index is 1, the material is at its liquid limit and is soft, whereas if the liquidity index is 0, the material is at the plastic limit, and is brittle (Murthy, 2002). The consistency of clay till and other clay-rich sediments is classified with respect to liquidity limit (see Tab. 2.1).

Table 2.1. The classification of clay-rich sediments with respect to the liquidity index (modified from Venkatramaiah, 2006).

Liquidity index, (I_L)	Consistency
<0.00	Very brittle
0.00 to 0.250	Brittle
0.251 to 0.50	Medium-soft
0.501 to 0.750	Soft
0.751 to 1.00	Very soft
>1.00	Liquid

2.2 Assessment of undrained shear strength from Atterberg limits and derived indices

Depending on the geological material being analysed, different test and calculation methods are applied to determine undrained shear strength. Although there are many studies that suggest shear strength estimations from liquidity and plasticity indices for clay, not many studies are available that are correlating shear strength and the described indices for clay till. Apart from the relations described above, an application of an appropriate cone factor (N_{kt}) is of interest, as this factor is used to calculate undrained shear strength from CPT. A part of estimations described in this section was applicable to the results gained in this study, and the test results are observed and discussed in subsection 6.5.

The assessment of shear strength from Atterberg limits is closely related to the development of empirical calculations of shear strength from both CPT and VST. Studies by Skempton and Northey (1952) and by Schofiled and Wrother (1968) led Wroth and Wood (1978) to propose a new equation to estimate shear strength from liquidity index for clayey sediments (Vardanega and Haigh, 2014).

$$c_u = 170e^{-4,6\,I_L} = 1.7 \cdot 10^{2(1-I_L)} \text{ (kPa)}$$

This equation indicates that the undrained shear strength should be 170 kPa at the plastic limit and 1.7 kPa at the liquid limit (Wroth and Wood, 1978).

Later, an alternative correlation was proposed by Leroueil et al. (1983) which is applicable for liquidity indices between 0.5 and 2.5:

$$c_u = \frac{1}{(I_L - 0.21)^2} \text{ (kPa)} \quad 0.5 < I_L < 2.5$$

where c_u is the undrained shear strength, e is a mathematical constant and I_L is the liquidity index.

Locat and Damers (1988) proposed an equation suited for sensitive clays with high liquidity indices:

$$c_u = \left(\frac{1.167}{I_L}\right)^{2.44} \text{ (kPa)} \quad 1.5 < I_L < 6.0$$

When estimating undrained shear strength from VST, the Bjerrum correction factor (μ) is applied as a constant value. Initially, Bjerrum (1954) stated that undrained shear strength in clays increases with depth, meaning that this relation can be expressed as a constant ratio of undrained shear strength to effective vertical stress. In later studies, Bjerrum (1973) suggested using a correction against the soil plasticity, known as the Bjerrum's correction factor μ, when calculating the shear strength in clay-rich sediments from VST:

$$c_u = \mu\, c_{uVST}$$

where μ is correction factor and c_{uVST} is a shear strength from VST.

Bjerrum suggested that the correction factor might be determined from the plasticity index (I_p) as the effects of anisotropy and strain rate on the shear strength were considered (Fig. 2.2)

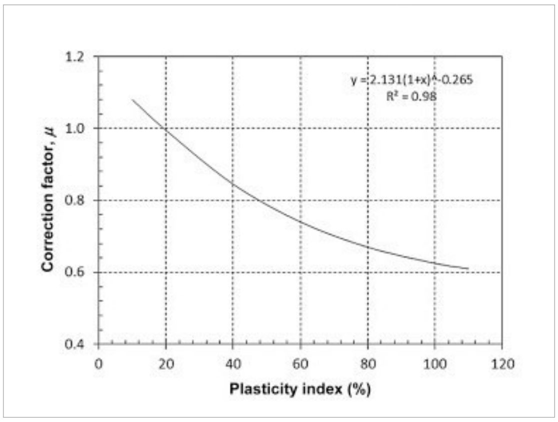

Figure 2.2. Bjerrum's correction factor with respect to plasticity index (Bjerrum, 1973).

In contrast, Dolinar (2010) did not find a constant criterion to determine the normalized undrained shear strength from the plasticity index for all clay-rich sediments, as the normalized undrained shear strength can only be correlated with the plasticity index for non-swelling clays.

Kayabali et al. (2015) suggested that the effect of plasticity on the undrained shear strength of clayey sediments is better represented when the measured undrained strength values are correlated with the liquidity index.

When calculating shear strength from CPT results, a constant value of cone factor (N_{kt}) is used to calculate the undrained shear strength:

$$c_u = \frac{q_t - \sigma_{v0}}{N_{kt}}$$

where q_t is a total cone resistance (cone resistance, corrected for pore pressure effects), σ_{v0} is the effective vertical stress and N_{kt} is the cone factor.

The Swedish Geotechnical Institute (SGI) suggests a constant value for the cone factor N_{kt} =11 (Larsson, 2015), which is used to determine the undrained shear strength of clay tills in Sweden. While a cone factor value of 11 (N_{kt}) is used in Sweden, a value of 10 is established and used in Denmark based on the tests of the Storebæltsbroen area (Steenfelt and Sørensen, 1995).

Luke (1996) found that the plasticity and the content of impurities in the material may influence both the friction ratio and the cone factor and suggested the following calculation for the cone factor:

$$N_{kt} = 15 \cdot R_f^{-0.4}$$

where R_f is the ratio between the sleeve friction (f_s) and the cone resistance (q_c), (%).

Young and Daehyeon (2011) suggested a new empirical equation for estimation of the cone factor in different counties in Indiana, USA:

$$N_{kt} = 0.285 I_P + 7.636$$

Aas et al. (1986), Young and Daehyeon (2011), Nwobasi and Egba (2013) found that the cone factor increases as the plasticity index rises, which conforms with some studies, while other researchers reported decreasing trends (Lunne et al., 1976). Luke (1994) in her study did not find any pronounced relation although it was found that the plasticity index and the plastic limit affect the cone factor.

In summary, since K. von Terzaghi discovered the potential of the Atterberg limits in soil mechanics, in 1925, many studies have been performed to correlate shear strength and liquidity and plasticity indices in clayey sediments, and several authors offered empirical shear strength calculations. Furthermore, different cone factors (with respect to both indices) and Bjerrum correction factors have been proposed to calculate shear strength from CPT and VST. The results have been inconclusive. While one research group found that the shear strength fits well with the liquidity and plasticity indices, other results contradict such a relationship and provide opposite results.

2.3 Previous studies on clay till

To carry out this thesis, a literature study of clay-rich sediments in Scania was conducted. The general development of southwestern Scania in connection with the new Öresund Link to Denmark has led to deeper knowledge of the local clay tills (Larsson, 2001). Therefore, diverse studies have been conducted in this area, while just a general description of the Simrishamn area was found in Daniel (1986).

Dueck (1998) and Larsson (2001) studied The latter authors describe the two different types of till referring to Baltic and Northeast tills, which are not geological terms and only indicate the provenance of clasts. Further in the text the Baltic clay till is named as Lund Till consistent with the terms used in other studies (Berglund and Lagerlund, 1981; Ringberg, 2003; Anjar, 2013). Lund Till is found from the ground surface down to 3 m depth and contains a large amount of sedimentary bedrock particles. The grain size distribution indicates that the Lund Till is a clay till or a sandy clay till (Fig. 2.3).

The groundwater level at Tornhill is situated 1.5 m below the ground surface (Dueck, 1998). A good correlation between plasticity index and the liquid limit of the Lund Till has been found (Dueck, 1995).

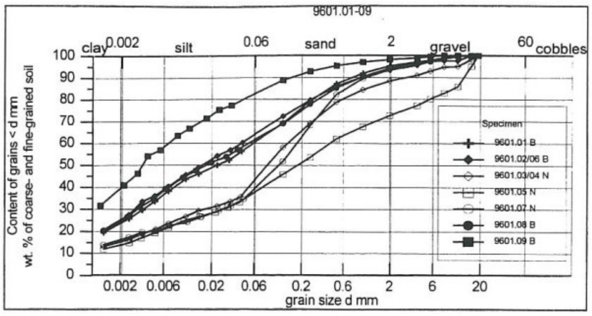

Figure 2.3. Grain size distribution for seven samples from Lund Till (Dueck, 1998).

To determine different properties of the Lund Till, a significant number of various tests were implemented by Dueck (1997) and Larsson (2001) (see Tab. 2.3).

*Table 2.3. The summary of different properties and undrained shear strengths of Lund Till. Modified from Dueck (1997, 1998) and Larsson (2001). * Plasticity index was estimated from a relation $I_P = 0.79\ (w_L - 0.12)$*

Properties	Lund Till (Dueck, 1997, 1998)	Lund Till (Larsson, 2001)
w %	14 - 21	13 - 17
w_L %	47	20 - 37
w_P %	19	13 - 16
$I_{P\,\%}$	-	8 - 12*
c_u (Triaxial)	175 - 350	165 - 175
c_u (CPT) kPa	50 - 400	30 - 400
c_u (VST) kPa	80 - 420	300 - 400

As it can be seen, physical properties of the Lund Till are quite close, while the undrained shear strengths scatter widely as not only the heterogeneity of the till but also sampling, the precision of measurements and other factors affect the results of undrained shear strengths.

Undrained shear strength from CPT showed that results scatter widely. However, a comparison between CPT and VST suggests that a cone factor between 10 and 12 would be appropriate (Larsson, 2001).

Jacobsen (1970) and Hartlén (1974) proposed undrained shear strength relations for clay till taking the void ratio (e_0), water content (w) and clay content (l_c) into account. However, the comparison with the measured undrained shear strengths from triaxial tests showed that estimated undrained shear strengths are mainly lower (Larsson, 2001).

A very detailed division of the tills by characteristic mineral composition has been performed by Ekström (1936, 1950), who states the shale-crystalline till is the most widespread till in Scania (Daniel, 1986; further discussed in section 6). Meanwhile, the division of clay tills by the percentage of clay particles is used to visualize tills in the Quaternary sediment map (Sveriges Geologiska Undersökning, 1985; Sveriges Geologiska Undersökning, 1987; Daniel et al., 2000; Ringberg, 1987).

3 Geology

3.1 Bedrock of Scania

The information presented in this section is based on maps and general descriptions from the National Atlas of Sweden (Sveriges Nationalatlas, 1999).

Scania is located at the boundary between the Baltic shield and the younger Central European sedimentary bedrock area. This unique location provides the variety of bedrock of Scania which formed between 1700 and 50 million years ago. The Precambrian bedrock mainly lies directly under the Quaternary deposits in the northern part of Scania and primarily consists of orto gneiss, gneiss-granite, syenite and monzonite. On the contrary, younger sedimentary bedrock, including sandstone, clay shale, limestone and claystone, and Quaternary deposits cover this older bedrock in the southern part (Fig. 3.1). The tectonic movements have developed the bedrock surface that is observed today. A wide tectonic zone, the Protogine Zone, divides the Precambrian bedrock into a western part consisting of mainly gneiss, and an eastern part consisting of volcanic rocks and granite. This zone stretches from the Romele Horst up to the county border in the north. Another, younger tectonic structure, the Tornquist zone, crosses Scania from northwest to southeast (see fault zones in Fig. 3.1). This zone began to develop during the younger Carboniferous-Permian Periods, and resulted in raised fault blocks (horsts) and

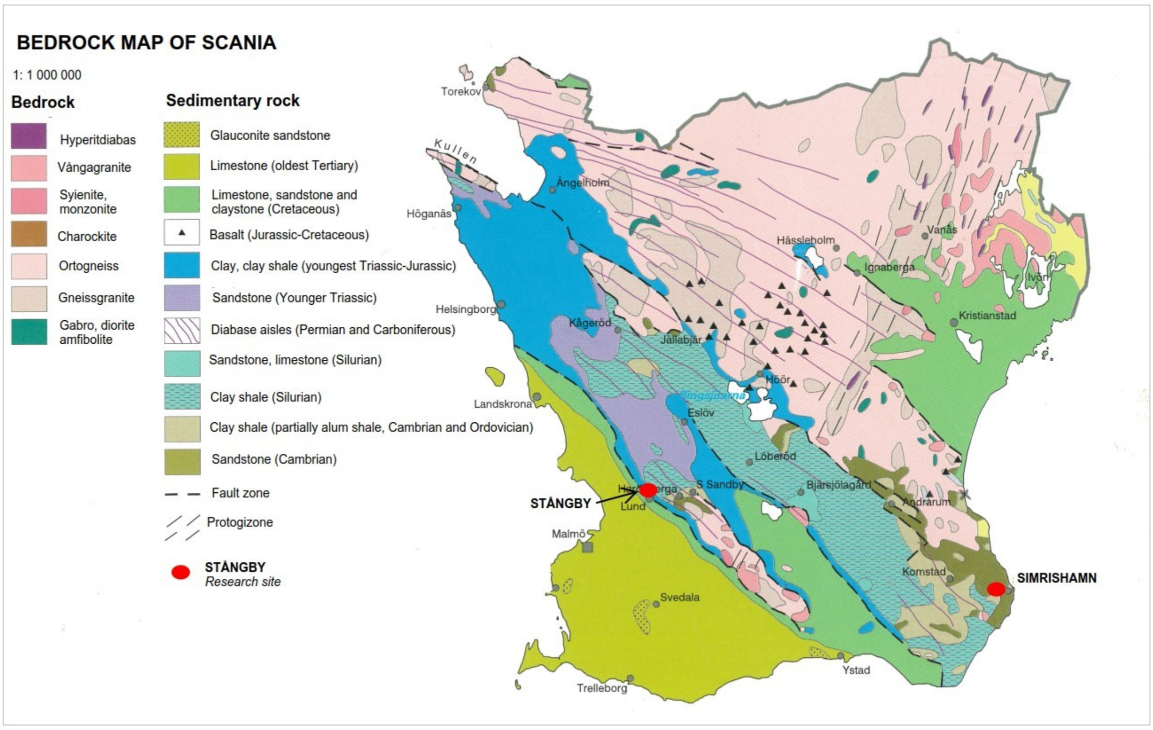

Figure 3.1. Map of the bedrock of Scania. Study sites are marked with red circles and names. Modified from Sveriges Nationalatlas (1999).

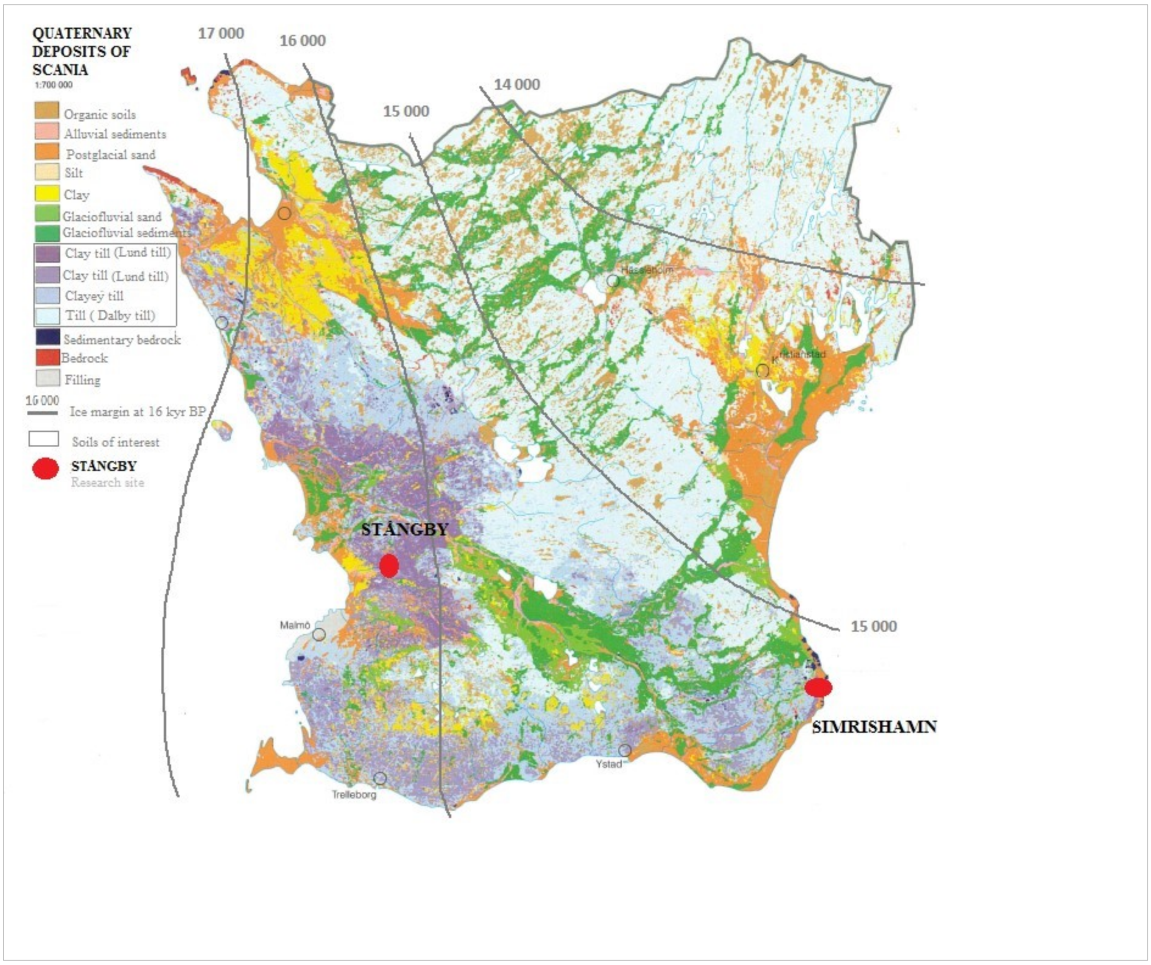

Figure 3.2. Map of Quaternary deposits in Scania and deglaciation recession from 17 to 14 kya BP. Study sites are marked with red circles and names. Modified from Sveriges Nationalatlas (1999).

subsided areas (grabens). These subsided areas are filled with clay, clay shale and sandstone from the Triassic-Jurassic Period, while only the higher Precambrian horsts are exposed at the surface.

During the Cretaceous-Neogene Periods, Scania was exposed to significant vertical movements which led to the development of smaller basins, such as the Kristianstad and Vomb depressions. A part of Scania around Kristianstad and the southernmost part of Scania, from Landskrona to Ystad down to the Falsterbo Peninsula, was covered by the sea and subsequently limestone was deposited. Today this limestone, rich in fossils, forms up to 1400 m thick sedimentary bedrock layer in the southern part of Scania and only up to 400 m around Kristianstad.

3.2 Quaternary deposits in Scania

The bedrock surface of Scania is covered by Quaternary deposits, with a thickness varying from a few to more than 130 meters, depending on bedrock surface undulations (Sveriges Geologiska Undersökning, 1980 and Sveriges Geologiska Undersökning, 2017). Where the bedrock surface is elevated, the Quaternary deposits are usually thin, whereas in depressions the thickness increases.

The Quaternary deposits are composed of till, glaciofluvial sands and gravel, glaciolacustrine fine-grained sediments, postglacial sand, clay, peat and gyttja. The deposition of the Quaternary sediments we observe today began in the Late Weichselian (25-11.7 kyr BP), when the Scandinavian ice sheet reached its maximum extent (ca 23 kyr BP; Fig. 3.3). Later ice sheet re-advanced and glacio-isostatic rebound during the following deglaciation period led to deposition of tills, gravel and sand, silt and clay.

When the Scandinavian Ice Sheet reached its maximum extent at 25-21 kyr BP it covered the province of Scania, the eastern part of Denmark and extended into the northern parts of central Europe. During this advance, the Dalby Till was deposited in Scania.

The deglaciation phase (20-15 kyr BP) was the next essential step in the geological development of Scania. At ca 20-17 kyr BP southern Sweden and Denmark were exposed to several re-advances, different studies give contradictory results regarding the deglaciation. At ca 17 kyr BP the ice margin had retreated along the Swedish west coast, and the Kullen Peninsula in northwest Scania is believed to have become ice-free for the first time (Sandgren et al., 1999; Fig. 3.3).

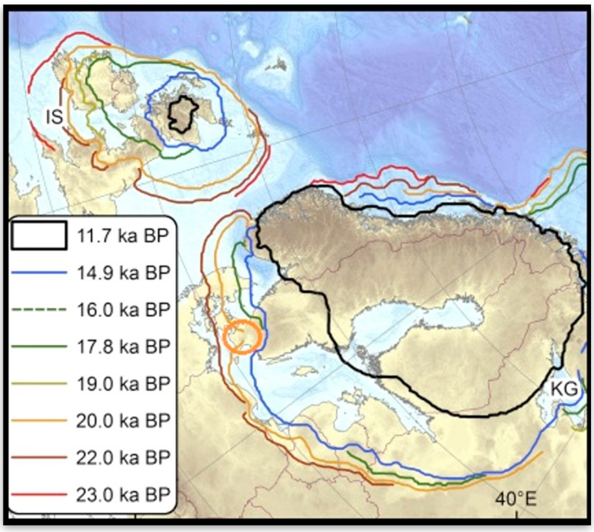

Figure 3.3.The maximum distribution of Scandinavian Ice Sheet during the Late Weichselian glacial period. The province of the Scania is encircled with orange. Modified from Patton et. al 2017.

The next phase in the deglaciation of Scania is characterized by the formation of periglacial surfaces and a last re-advance (Anjar, 2013). The deglaciation was interrupted by the last Öresund re-advance (ca 17 kyr BP) of the Young Baltic Ice stream, which extended over southwestern Scania to south and west of the Romele Horst, depositing the Lund Till (Ringberg, 2003; Anjar, 2013; Anjar et al., 2014; Houmark-Nielsen and Kjær 2003). As the ice sheet was thin, and shortly after advancing vast territories in low-lying areas along the south and west coast of Scania became ice free.

3.3 Clay tills at the Stångby and Simrishamn sites

During tens of thousands of years, Scania experienced several glacier advances from different directions, and clasts of various origin were incorporated in the sediments and later deposited by glaciers. Ekström (1936) studied tills in Scania and divided them into several areas based on the characteristic mineral clasts incorporated (Fig. 3.4).

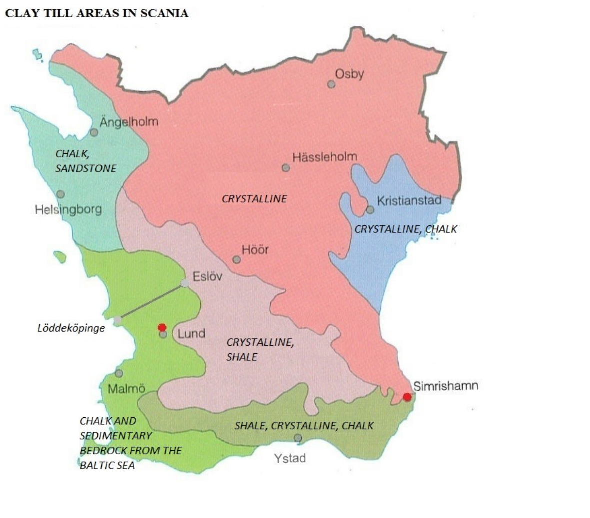

Figure. 3.4. Areas of clay tills in Scania. Study sites are marked with red circles. The cross-section between Löddeköpinge and Eslöv cities is marked with a grey line. Modified from Ekström (1936).

As can be seen the chalk and sedimentary bedrock clasts are typical for the till in the southwestern part of Scania (light green area in Fig. 3.4). Ringberg (1987) describes that the till rich in clay and chalk lies in southwestern Scania and its thickness varies from 1 to 20 m. A cross-section in west-southwest to east-northeast directions shows that clay till is mainly the thinnest in the western part (approx. 1m) and increases in thickness (up to approx. 20 m) as it approaches the border of its distribution. This sketches the noticeable borders in the Quaternary map (Ringberg, 1987; Sveriges Geologiska Undersökning 1987). The clay content in the clay-rich till generally varies between 25 and 40%, but might reach up to 40 to 60%, occasionally surpassing 60% (Fig. 3.5).

The clay-rich till also lies in a narrow area along the coastline near Simrishamn. It is assumed that two potential processes might have contributed to the high clay content. From one side, it is believed that either this clay-rich till has formed by reworking sedimentary clay, or by the weathering of chalk and limestone of the uppermost part of the till.

The same phenomenon is observed in southwestern Scania (Daniel, 1986). Ringberg (2003) and Anjar (2013) concluded that the clay-rich till was deposited by the Öresund re-advance by the Young Baltic Ice stream ca 17 kyr BP.

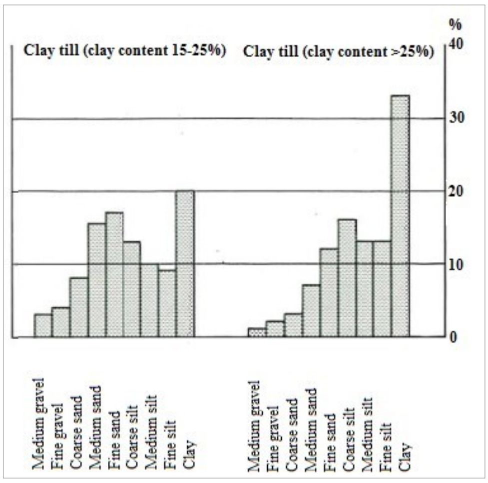

Figure 3.5. The grain-size distribution of clay tills at Stångby (right) and Simrishamn sites (both images) according to Quaternary deposit maps SGU 1987; SGU 1985. Modified from Ringberg (1987).

In contrast, the Simrishamn site lies on the border of two till areas: the one till includes crystalline mineral clasts while the other has shale and chalk (red/dark green area in Fig. 3.4). Moreover, the whole Simrishamn area represents the very shifting thickness of Quaternary sediments being dependent on the morphology of the underlying sedimentary bedrock (Cambrian sandstone); the till cover is missing almost completely west and northwest of Simrishamn (Daniel, 1986).

3.4 Field site geology

The digital map generator allows us to gain information about the Quaternary deposits at the Stångby and Simrishamn sites from the website of the Geological Survey of Sweden (Sveriges Geologiska Undersökning kartvisare, 2018a and 2018b) (Fig. 3.6 and 3.8). Since the sites vary greatly in size, different scales were used in the maps. The legend for both maps is found below the Stångby map.

3.4.1 Site I - Stångby

The Stångby area is located approximately 3 km north of Lund and lies approximately 45 m above sea level. The investigation area is dominated by cultivated land.

According to the website of the Geological survey of Sweden (Sveriges Geologiska Undersökning) digital map (Sveriges Geologiska Undersökning kartvisare, 2018a) clay till with a clay content >15 % overlies the sedimentary bedrock and forms up to 10 m thick Quaternary sediments (Sveriges Geologiska Undersökning, 2018a; Sveriges Geologiska Undersökning, 2017) (Fig. 3.6.).

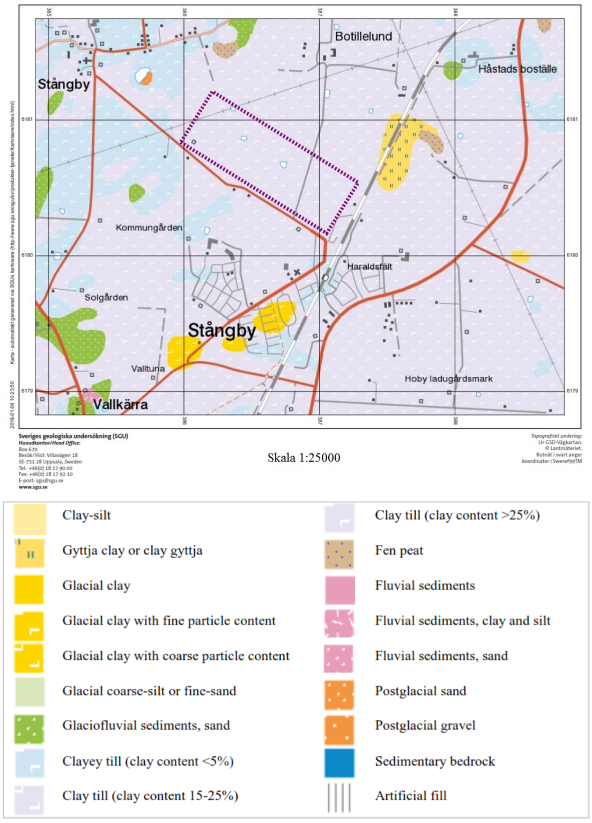

Figure 3.6. The study site at Stångby is marked with a purple dashed line. Modified from SGU (2018a).

Geological investigations (Tyréns, 2017a) show that a clay till rich with humus lies 0.0-0.3 and 0.0-0.8 m deep, overlies clay till which lies approximately to a depth of 1.8 m (Fig. 3.7, 6.1, 6.2.).

Figure 3.7. Clay till with chalk clast at Stångby. Photo by the author, 2018

Below these two layers, a clay till with occasionally embedded 30 to 60 cm thick sand lenses is situated at 1.8-4.0 m depth. This separate clay till with sand lenses was found only at the three points located in the western part of the site and was not included in this study.

3.4.2 Site II - Simrishamn

Compared with Stångby, the Simrishamn site is a small area located in the middle of Simrishamn city. A clay till with a clay content of 15-25% dominates the area (Fig. 3.8 and the labels under 3.6.).

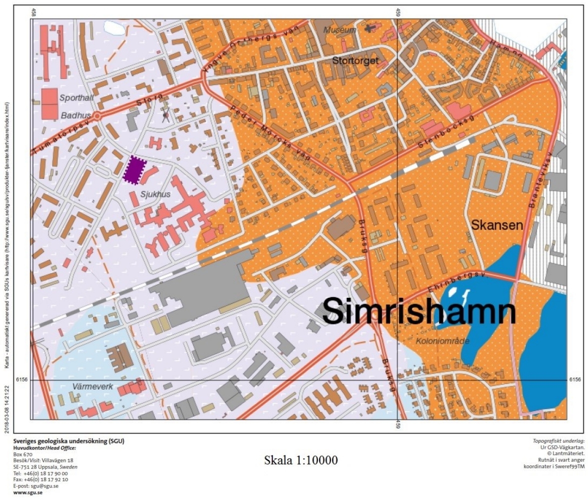

Figure 3.8. The study site at Simrishamn is marked with a purple square. Modified from SGU (2018b)

This till overlies the Cambrian sandstone, which lies approximately 10 m deep (Sveriges Geologiska Undersökning, 2018b; Sveriges Geologiska Undersökning, 2017; Sveriges Geologiska Undersökning, 1985). Apart from that the clayey till areas with a clay content lower than 5% (light blue areas in Fig. 3.8) were found near the study site, and vast fields with postglacial sand and gravel (orange areas) cover the coastal areas and parts of the city.

Geological investigations (Tyréns, 2017b) shows that the medium sand overlies brown, sandy and silty clay till which is situated at 0.7 - 3.6 m depth (Fig. 3.9 left). Below this clay till, a brown silt layer is underlied by grey clay at 3.6 - 4.0 m depth. A grey clay till lies at the base of the borehole 4.0 - 6.0 m depth (Fig. 3.9 right).

Figure 3.9. A sandy, silty brown clay till (left) and a clay-rich, grey clay till (right) with clasts from Simrishamn site. Photo by the author, 2018

4 Methods

In this study, several field and laboratory methods were applied to collect samples, analyse physical properties and determine undrained shear strength of clay tills from Stångby and Simishamn. Test standards and guidelines of the Swedish Standard Institute were followed. To obtain test samples, disturbed sampling was accomplished with a GeoTech 604 drill rig. CPT no. 4907 and CPT 4933 were used to implement cone penetration tests and the Danish vane V5 type was used for vane shear tests and to calculate the undrained shear strength. Considering field descriptions of the previous studies and various limitations of the equipment, a maximum depth of 2.0 m at Stångby and 5.9 m at Simrishamn was reached in this study. Altogether 12 disturbed samplings, 10 CPT soundings and 11 field vane tests at 8 points were performed at the Stångby site from 0.3 to 2.0 m depth (see Tab. 4.1).

Table 4.1. The summary of test methods performed in this study

Site	Disturbed samples	CPT points	VST points
Stångby	12	10	11
Simrishamn	11	3	-

Both the 11 disturbed samplings and CPT were conducted at 3 points from 1.2 to 5.9 m depth at the Simrishamn site. Results from VST and CPT were analysed for the same sampling depth. Disturbed samples were obtained for further determination of Atterberg limits: the liquid limit and the plastic limit, and related indices. To calculate both plasticity and liquidity indices, the percentage of natural water content was also determined. In addition to the investigation methods mentioned above, many empirical calculations were tested, as undrained shear strength estimation from Atterberg limits has been of interest since 1925 (Terzaghi, 1925). Finally, the results were mainly displayed in graphs and the correlations between shear strength and liquidity and plasticity indices were estimated using either linear or exponential regressions.

4.1 Field methods

4.1.1 Disturbed sampling

The most common method for sampling is a disturbed sampling. While the basic methods include sampling from the test pits or with a hand auger, more advanced sampling with a drill rig provides disturbed sampling from greater depths. In this study a screw auger mounted on a drill rig was used for obtaining the disturbed clay till samples. The screw auger is a sampler designed as a screw on a steel rod and the diameter varies from 30 to 200 mm, although a diameter of 60 to 100 mm and 1 m height is most frequently applied (Svenska Geotekniska Föreningen (SGF), 2013; see Fig. 4.1.left).

Figure 4.1. The screw augers of the different sizes, (left, SGF, 2013); a drill rig with the lifted screw auger (right). Photo by the author (2018)

The screw auger is primarily used for clay-rich sediments down to 5 m depth, although drilling down to 15 m is possible. During sampling, the auger is screwed into the ground to the desired depth and then pulled out (Fig. 4.1.right).

The clay till remains on the ribs of the auger as it is pulled out, representing the geological profile of the depth interval (Svenska Geotekniska Föreningen, 2013). Finally, clay till samples are carefully taken and placed in plastic bags and the boring number and the depth of the samples are noted. Notes are made in a field book including simple descriptions of the clay till samples.

4.1.2 Cone penetration tests

When performing a CPT sounding, a cylindrical probe with the total cross-sectional area of 1000 mm^2 and a cone with 60° apex angle is pushed into the ground with a constant rate of 20 mm/s. During the test the following quantities are measured: cone resistance (q_c), sleeve friction (f_s) and pore pressure (u) which is measured in a porous ring between the cone and cylinder (Larsson, 2015)(see Fig. 4.2).

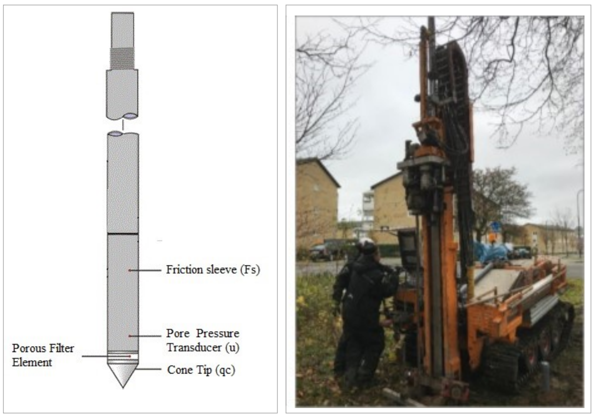

Figure 4.2. A cone penetration probe (left), modified from Larsson, (2015) and a CPT equipment in use at Simrishamn (right). Photo by the author (2017)

Typically, CPT sounding is a complementary method for disturbed sampling in the field and principally constructed to ascertain the ground profile. However, sounding also gives information about continuous shear strength variations in the sediments (Svenska Geotekniska Föreningen, 2017), and this is a method widely used in Sweden. CPT is used to a large extent to empirically calculate undrained shear strength. Alternatively, a dynamic penetration test can be applied as this method is adjusted to a coarser material. However, its main aim is to determine the ground profile (Swedgeo, 2017). Sounding results are influenced by various conditions, like particle size, density, overburden and horizontal stresses in the layer. Therefore, CPT sounding data should be regarded as complex, considering relations and variations of all three measured features: cone resistance (q_c), sleeve friction (f_s), and pore pressure (u). For example, the coarser the material is, the higher is the cone resistance and the lower friction ratio (R_f) (a relation between cone resistance and sleeve friction) and lower pore pressure. The undrained shear strength usually is calculated using measured cone resistance (q_t) values, and effective vertical stress (σ_{v0}):

$$c_u = \frac{q_t - \sigma_{v0}}{N_{kt}} \text{ (kPa)}$$

where q_t is the total cone resistance, σ_{v0} is the effective overburden stress, and N_{kt} is the cone factor (Larsson et al., 2007).

4.1.3 Vane shear tests

The vane shear test is a simple in-situ method to determine the shear strength of soft to medium brittle clays. This method is widely used in geotechnical investigations due to its time and cost effectiveness and simplicity. Moreover, the VST enables measurement of the undrained shear strength at a certain point, thus it is used as a complementary method to validate CPT sounding results (Svenska Geotekniska Föreningen, 2017). A Swedish field vane is designed for soft clays and considered not to be suitable to measure the shear strength in clay tills. The Danish vane instrument is more appropriate due to its design, which was created on a basis of surveying firm clay tills in Denmark (Larsson, 2001; Fig. 4.3).

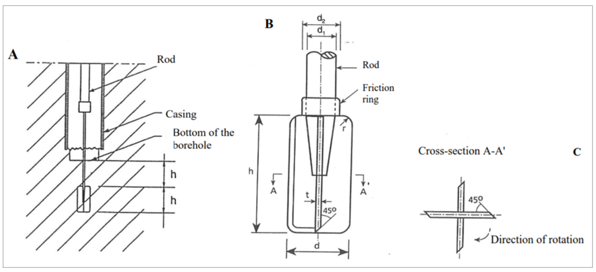

Figure 4.3. A - a schematic picture of the Danish field vane; B - the geometry of the vane; C - the cross-section. Modified from Dansk Geoteknisk Forening, 1998

Since the Lund Till in southwest Scania and Denmark was formed during the same ice advance, the Danish vane instrument is broadly used in geotechnical investigations in southwest Scania.

The Vane instrument consists of a four-bladed vane which is mounted on a cylindrical rod. To reach the required depth, the holes are pre-bored and then the VST probe is lowered at the bottom of these pre-bored holes. A rod is pushed into the undisturbed sediment until the base of the vane reaches a depth up to twice the height of the vane (see Fig 4.3A). Next, a torque wretch is attached to the rod and slowly rotated until the moment at which the sediments reach failure.

Although the operating principle is the same, various vane sizes are used depending on the expected undrained shear strength. Vane types V4, V5, HVA and HVB are used down to 20 cm depth from the bottom of the borehole, while V7.5 and V9.2 are used approximately down to 30 cm depth from the bottom of the borehole (Dansk Geoteknisk Forening, 1998). For vanes V4 and V5, a repetition of the shear test procedure can be made at 20 cm depth from the first test point. To implement vane shear test at Stångby, the V5 type Danish vane instrument was used (see Tab. 4.2).

Table 4.2. Measurements of different Danish vanes, vane load capacity and a constant applied to undrained shear strength calculations. Modified from Dansk Geoteknisk Feltkomité, 1998.

Type	**h (mm)**	**d (mm)**	**r (mm)**	**$c_{v,\,max}$ (kPa)**	**M(m^3) (constant)**
V4	80	40	10.0	715	$0.2097\cdot10^{-3}$
V5	100	50	12.5	366	$0.4096\cdot10^{-3}$
V7,5	150	75	18.8	109	$1.3820\cdot10^{-3}$
V9,2	350	92	23.0	32	$4.7588\cdot10^{-3}$
HVA	66	33	7.0	333	$0.1201\cdot10^{-3}$
HVB	96	48	10.0	108	$0.3703\cdot10^{-3}$

Next, the measured peak torque was used to calculate the vane strength (c_v):

$$c_v = \frac{P_a}{M'} \text{ (kPa)}$$

where P_a is a peak torque (Nm) and M' is a constant (m^3), depending on the dimensions and shape of the field vane (Dansk Geoteknisk Forening, 1998). It is considered that the vane strength value measured in the clay till is about the same as the undrained shear strength value, thus:

$$c_v \approx c_u \text{ (kPa)}$$

4.2 Laboratory methods: liquid and plastic limits

To implement laboratory tests, the informational booklet of the Swedish Geotechnical Institute (Larsson, 2008) and the Swedish Standard (Swedish Standards Institute, 2008) were followed. At the initial phase, the natural water content of each sample was determined. First, a specimen was taken out of the bag, weighted and put into the oven at 105°C to dry out for 24 hours. Next, the sample was taken out of the oven and weighed again (Larsson, 2008).

The liquid limit was determined by the fall cone method. A paste of moisture sediment was put in a bowl and inserted into a fall cone device. A cone with a mass of 60 g and tip angle of 60° was lowered until it almost reached the surface of the sample and then released (Fig. 4.4).

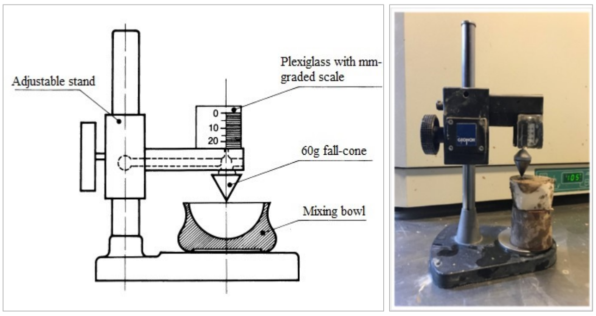

Figure 4.4. A schematic image of the fall cone device (left), modified from Larsson, 2008; and the fall cone in use (right), photo by the author (2017).

When the cone had dipped, the cone imprint was measured and the liquid limit was calculated according to guidelines of Swedish Geotechnical Institute (Larsson, 2008).

The plastic limit, also called a rolling limit, is the lowest water content in the sample at which it retains its physical ability to be rolled out to a 3 mm thick thread without falling apart. The water content was calculated according to Swedish standard (Swedish Standards Institute, 2014) and the result obtained was determined as the plastic limit.

5 Results

The relationship between the liquidity index (I_L) and the undrained shear strength (c_u) was tested for clay tills from the two sites in Scania. To visualize and analyse the undrained shear strength with both plasticity (I_P) and liquidity indices the determined indices were attributed to the whole disturbed sample and the point values of the shear strength at the particular depths were extracted from CPT and VST measurements. The analysis of the liquidity index and the undrained shear strength was combined with empirical estimations from the previous studies described in the subsection 2.2.

5.1 Site I - Stångby

Results from the Atterberg tests show that the liquidity index (I_L) in the clay till samples varies from -0.10 to 0.34 with only one sample having a negative value (see Tab. 5.1). The average value of 0.22 indicates that according to the consistency classification, Lund Till at Stångby can be generally classified as having a very brittle to brittle consistency (Tab. 2.1).

The undrained shear strength obtained from the two methods shows different values: while $c_{u\mathrm{CPT}}$ varies between 57 and 256 kPa, the $c_{u\mathrm{VST}}$ shows lower values, between 42 and 208 kPa. Interestingly, the average values from the two methods are very close, 126 and 125 kPa respectively.

5.2 Site II - Simrishamn

The liquidity index of 8 samples from Simrishamn varies between -0.35 and 0.23 and has primarily negative values (see Tab. 5.2). With an average liquidity index of -0.07, the clay till is classified as a having very brittle consistency (Tab. 2.2). The undrained shear strength calculated from CPT varies between 179 and 763 kPa with an average value of 337 kPa. It should be pointed out that an undrained shear strength higher than 350 kPa is more typical for frictional rather than cohesive sediments.

6 Analysis and discussion

6.1 Liquidity and plasticity indices at Stångby and Simrishamn

Firstly, there is no systematic change in the natural water content (w) with depth at both Stångby and Simrishamn sites (Fig. 6.1), and a higher variation of natural water content was found at the Simrishamn site than at the Stångby site. Secondly, as the liquidity index is directly dependent on the natural water content, no relation was observed when the liquidity index was plotted against depth (Fig. 6.2). At the Stångby site, the highest and lowest I_L values were found at the same depth of 1.1 m. In addition to I_L, I_P does not show any change with depth either.

Table 5.1. A summary from the Stångby site. Extremely high N_{ke} and c_{uCPT} values, and low c_{uVST} value are marked in yellow.

ID	Soil sample depth, m	Liquidity index, *IL*	Plasticity index, *IP*, %	Natural water content, *w*, %	VST depth, m	Undrained shear strength *cu*, kPa from VST	Total cone resistance, *qt*, kPa from CPT	Undrained shear strength cu, kPa from CPT	Empirical cone factor, *Nke*	Net tip resistance (qt-σv0) kPa
M1719	1.0-1.5	0.29	5.10	16.20	1.00	42	1251	112	30	1229
M1716	1.0-1.5	-0.10	10.61	12.20	1.10	208	2313	208	11	2289
A1768	0.3-1.0	0.24	17.82	18.90	0.70	93	910	81	10	895
		0.24	17.82	18.90	1.00	115	919	82	8	897
1709	0.3-1.0	0.29	20.43	18.00	0.70	100	1225	110	12	1210
	1.0-2.0	0.26	18.58	19.60	1.10	137	651	57	5	627
M1701	1.1-1.3	0.34	17.42	20.60	1.10	186	1093	97	6	1069
1703	1.6-1.8	0.25	21.63	17.60	1.70	101	2124	190	21	2087
1704	0.6-.,8	0.14	19.35	17.70	0.70	105	2832	256	27	2817
	1.0-1.3	0.21	19.90	19.30	1.20	135	808	71	6	782
1712	1.1-1.3	0.21	13.50	16.70	1.20	169	1193	106	7	1167
MIN		-0.10	5.10	12.20		42	651	57	5	627
MAX		0.34	21.63	20.60		208	2832	256	30	2817
AVG		0.22	16.56	17.79		126	1393	125	13	1370

Table 5.2. A summary from the Simrishamn site

ID	Soil sample depth, m	Liquidity index, IL	Plasticity index, IP, %	Natural water content, *w*, %	CPT depth, m	Total cone resistance, *qt*, kPa	Undrained shear strength, *cu*, kPa from CPT	Net tip resistance (qt-σv0)
17T01	2.2-2.4	-0.35	2.79	13.69	2.30	8443	763	8443
	5.7-5.9	0.12	13.86	19.62	5.80	2854	248	2854
17T02	1.2-1.4	0.23	14.40	22.14	1.30	2000	179	2000
	1.7-1.9	-0.21	5.50	18.85	1.80	3352	301	3352
	2.1-2.3	-0.07	11.51	19.82	2.24	2729	224	2729
	5.3-5.6	0.05	25.10	24.40	5.46	2622	227	2622
17T04	2.16-2.3	-0.29	5.91	12.16	2.20	2729	444	2729
	3.7-3.9	-0.05	6.80	23.10	3.80	2622	313	2622
MIN		-0.35	2.79	12.16		2000	179	2000
MAX		0.23	25.10	24.40		8443	763	8443
AVERAGE		-0.07	10.73	19.22		3419	337	3419

Several factors affect the variability of the indices. First, Skempton (1984) found that the plasticity of clay increases linearly with the percentage of the clay-size fraction. Therefore, the plasticity index directly demonstrates the composition of the clay till: the higher the I_P value, the higher the clay percentage of deposits, independent of depth. Second, I_L is dependent on the sediment composition and the water content.

It is common that clay-rich sediments above the groundwater table are saturated, and this is related to the capillary rise. The height of the capillary rise depends on the grain size and the size of pores in the material: for coarse sand the capillary rise is 0.03 to 0.12 m, while for clays it is more than 8 m (Larsson, 2008). Results from groundwater monitoring at Stångby from the 4-year period indicate yearly variations of the groundwater table: the highest level is observed from February to May and the lowest level is reached from August to October (Tyréns, 2017a). In this study groundwater table varies between 0.2 and 3.67 m depth. Therefore, it is expected that the natural water content of the clay tills might be higher from February to May, which might increase I_L at both study sites to some extent.

To summarize, the plasticity index is dependent only on the clay content of the sediments, whereas the liquidity index is affected by both the plasticity index and the natural water content. It is expected that the rise of the groundwater table during February to May will increase the natural water content of the clay tills,

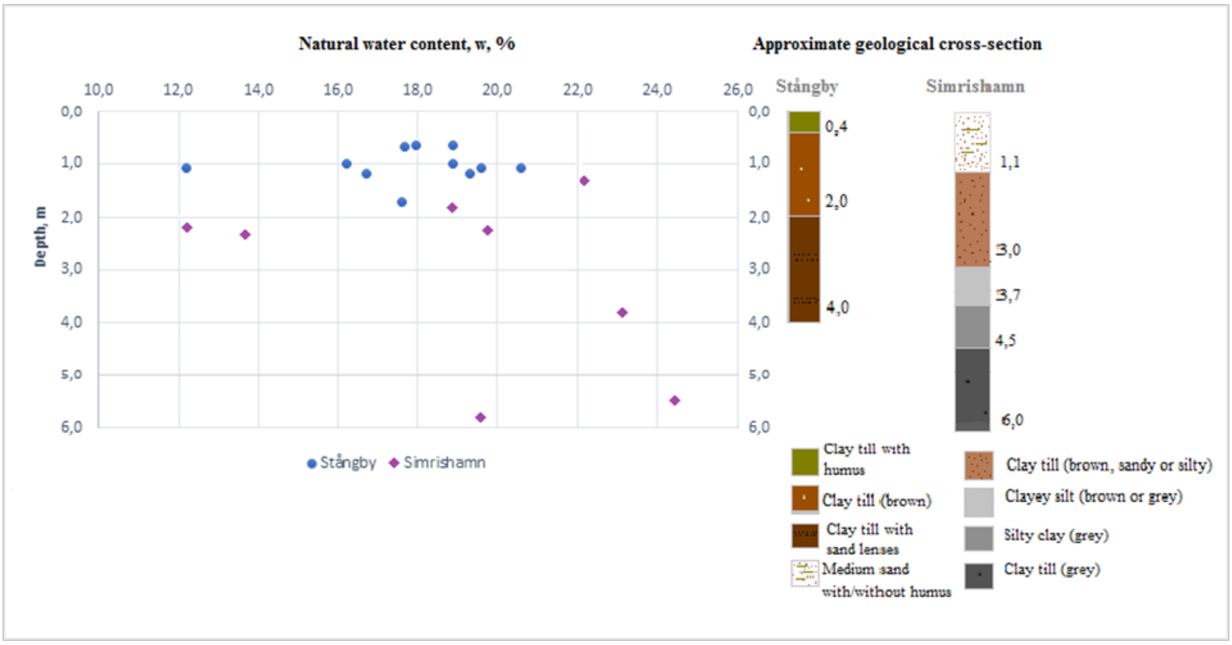

Figure 6.1. Variations of natural water content with depth

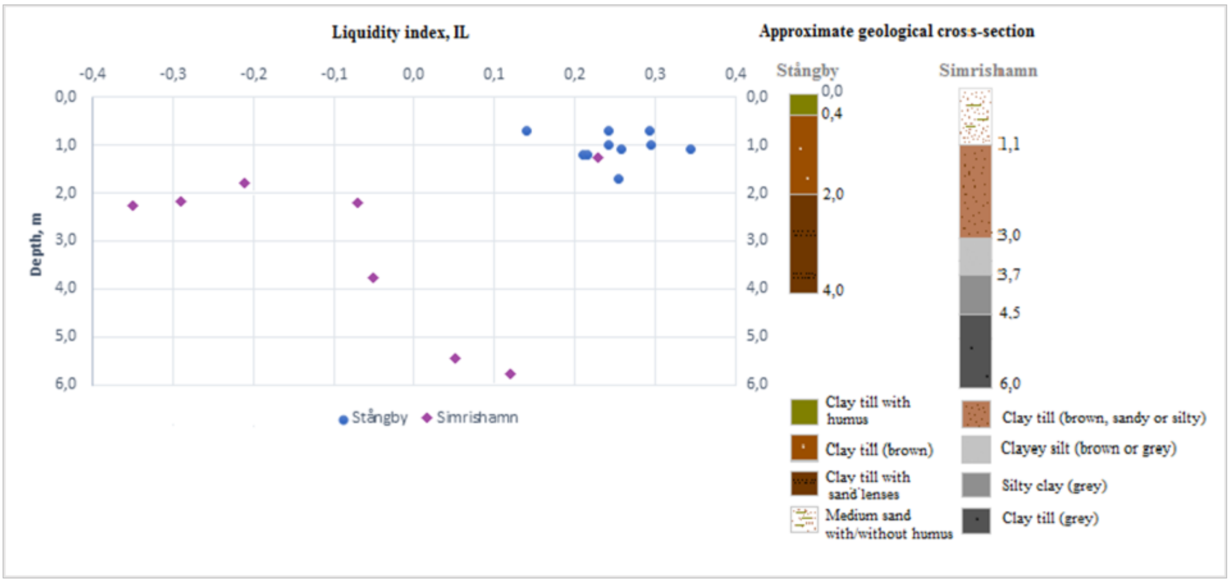

Figure 6.2. Liquidity index plotted against depth at the Stångby and Simrishamn sites

which in turn would result in the slightly higher liquidity index values, considering that the plasticity index is the crucial variable which provides a major impact on the liquidity index.

6.2 Liquidity index and undrained shear strength at Stångby

The shear strength values from the CPT and VST methods are scattered differently, between 199 and 166 kPa range respectively (see maximal and minimal undrained shear strength values from the CPT and VST in Tab.5.1.). This suggests that the CPT might be more susceptible to inhomogeneities of clay till than VST, giving occasionally higher cone resistance values and, consequently, higher undrained shear strength values. As Mayne et al. (2009) describes, the general difference in the shear strength is due to the different methods.

Related to this, Rémai (2012) describes that the measured undrained shear strength depends on the test method, the strain rate and many other factors. Also, Karpovics (2010) points out that the geotechnical behaviour of clay till is influenced by granulometric composition, the state of the consolidation, soil texture, deposition, conditions of sedimentation and post-sedimentation changes. Finally, CPT and VST measurements in this study were performed within a small distance (ca 30 cm) from each other, which also leads to different shear strength values.

The results from Stångby show that the undrained shear strength is higher in the very brittle consistency zone and decreases when the liquidity index slightly increases (Fig. 6.3).

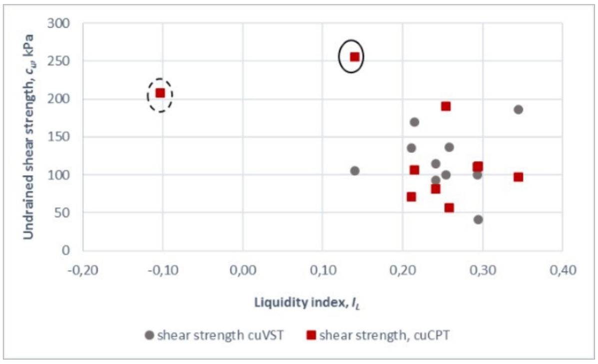

Figure 6.3. Undrained shear strength and liquidity index relationship at Stångby; An extremely high c_{uCPT} value is encircled with a solid and the only one negative I_L value is encircled with a dashed circle.

This would confirm a common knowledge of the soil mechanics, which states that the higher the water content, the higher the liquidity index and the lower the density of the sediments should be. Therefore, the lower the density is, shear strength should also be lower. However, it is very important that no relation can be found when an extreme value of c_{uCPT} and the only one negative liquidity index value are excluded.

With respect to the classification to liquidity index, in principle, all results lie in the brittle consistency zone

(I_L from 0.2 to 0.3) and the undrained shear strength varies mainly from 50 to 200 kPa.

It is assumed that the lack of direct measurements of the shear strength and a constant cone factor value of all clay tills lead to some level of uncertainty of the calculated shear strength from the cone penetration test. The cone factor, (N_{kt}) which is a constant of 11, is used to calculate the shear strength from CPT, not considering the inhomogeneity of the clay till (Larsson, 2015):

$$c_u = \frac{q_t - \sigma_{v0}}{N_{kt}} \text{ (kPa)}$$

where N_{kt} is the cone factor, q_t is the total cone resistance and σ_{v0} is the vertical stress.

Thus, the constant of 11 applied to the whole clay till layer may provide incorrect shear strength values.

The results from VST were used to back-calculate the cone factor for each point of interest:

$$N_{ke} = \frac{q_t - \sigma_{v0}}{c_{uVST}}$$

where c_{uVST} is the shear strength from vane shear test.

The empirical cone factor values vary from 4.6 to 29.6 with a general assemblage between 5 and 10 and an average value of 12.8 for 11 points (Tab. 5.1). The great variation of cone factor values suggests an individual assessment of the bulk density (ρ, kg/m^3) for each sample since bulk density is used in the determination of the unit weight (γ, kN/m^3) when estimating the shear strength from cone penetration test:

$$\rho = \frac{m}{V}$$

where m is the weight of the sediment sample (kg) and V is a volume of the sample (m^3);

$$\gamma = \rho g$$

where ρ is the density of the material (mass per unit volume, kg/m^3) and g is standard gravity (m/s^2) = 9.81 m/s^2.

Aas et al. (1986), Young and Daehyeon (2011) and Nwobasi and Egba (2013) found that I_P increases as N_{ke} increases, whereas later studies do not confirm this tendency. Neither the relation described above, nor the one between I_L and N_{ke}, was found in this study.

While there is no relation between N_{ke} and the two indices, the empirical cone factor correlates weakly with the net tip resistance (q_t-σ_{v0}) (Fig. 6.4).

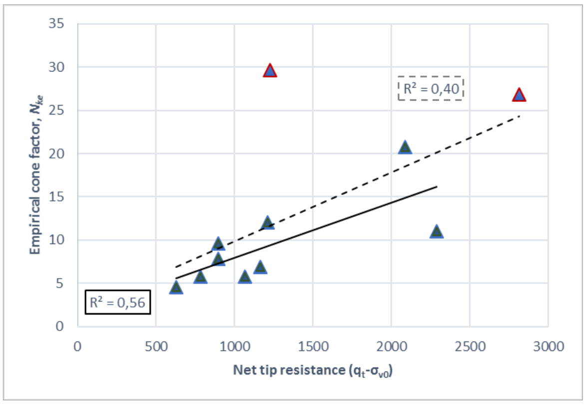

Figure 6.4. The empirical cone factor (N_{ke}) and net tip resistance (q_t-σ_{v0}); two extremely high cone factor values are marked with a red outline. The dashed linear regression line includes all points, while the solid regression line excludes the two extremely high values.

The relation with all empirical cone factor values (blue triangles) shows a slight fit (coefficient of determination R^2= 0.40), although after the elimination of the extremely high cone factor values (triangles with red outline), the relation shows better fit (R^2 = 0.56 Therefore, this might indicate that the N_{ke} is dependent on the total cone resistance, and to get correct c_u values, q_t should be divided by higher N_{ke} values. Concerned about the influence of the cone factor on the undrained shear strength results from CPT, many researchers have conducted their own studies with the aim to present different cone factors, either applicable locally or to a particular sediment type. A few of them, appropriate to this study, are discussed in subsection 6.5.

6.3 Liquidity index and undrained shear strength at Simrishamn

The results show that undrained shear strength varies between 179 and 763 kPa limits and the undrained shear strength tends to diminish when liquidity and plasticity indices increase. It is clearly seen that the undrained shear strength correlates better with the liquidity index (R^2 = 0.76) than with the plasticity index (R^2 = 0.49) (Fig. 6.5 and 6.6).

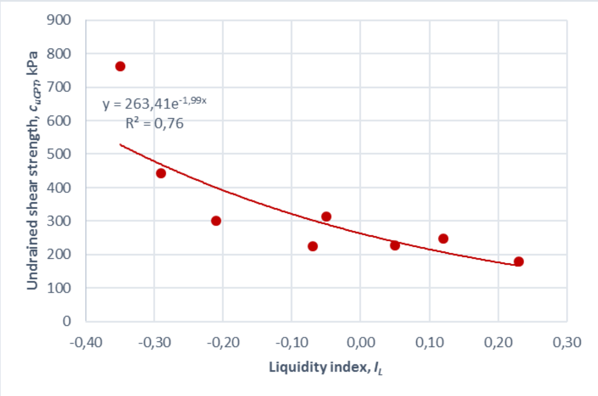

Figure 6.5. The liquidity index (I_L) and the undrained shear strength (c_{uCPT}) relationship expressed with an exponential regression line.

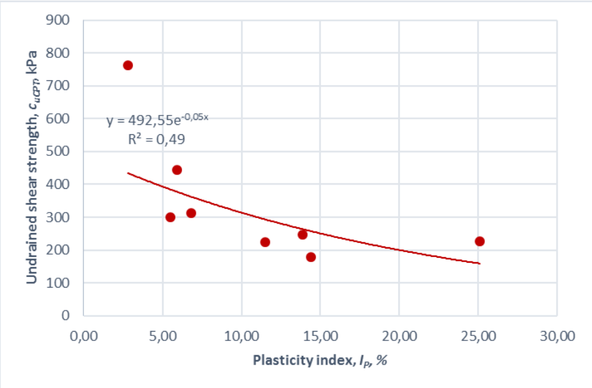

Figure 6.6. The plasticity index (I_P) and the undrained shear strength (c_{uCPT}) relationship expressed with an exponential regression line.

Therefore, Kayabali et al.'s (2015) hypothesis, that the effect of plasticity on the undrained shear strength of clay-rich sediments is better represented when measured undrained strength values are correlated with the liquidity index, was confirmed.

6.4 Liquidity index and undrained shear strength at Stångby and Simrishamn

When comparing the undrained shear stregnth from both sites, it is noticeable that shear strength values at Simrishamn are higher and vary within the 584kPa range from 179 to 763 (Tab.5.2.), whereas at Stångby they vary only within the 199kPa range (from 97 to 256 kPa, Fig.6.7 and Tab.5.1). In Parallel to observations in the laboratory, this provides additional evidence of the higher variability of the proportion of clay at Simrishamn, while clay till at Stångby can be considered as more homogeneous.

Apart from the low variability of the shear strength, the liquidity index also shows generally similar values varying from -0.10 to 0.34 at Stångby, which, unfortunately, resulted in a data assembly with no correlation. Although the coefficient of determination for both

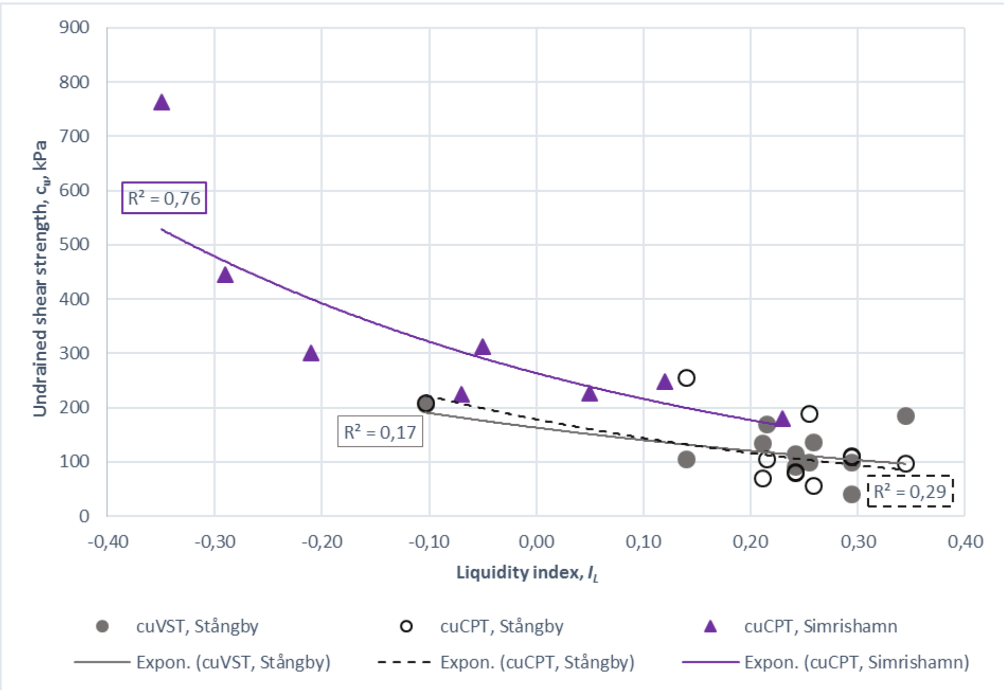

Figure 6.7. A summary of undrained shear strength and liquidity index from both Stångby and Simrishamn expressed by the exponential regression lines.

c_{uCPT} and c_{uVST} shows some relation, no relation is observed when the data set is evened out, suggesting that the undrained shear strength cannot be estimated if I_L values are closely distributed within one consistency zone (Tab.2.2.).

On the contrary, a quite pronounced correlation was found at Simrishamn, implying that the composition of the clay till contributes to a significant variation of I_L and c_{uCPT} (Fig 6.5). The low clay and natural water content of clay till lead to negative values of the liquidity index. A steep increase in the shear strength is observed in the very brittle consistency zone. The relation between q_c and I_P shows that I_P is the conclusive variable, which affects q_c, displaying higher q_c and lower I_L values for clay till with sandy impurities in comparison with those with the higher clay content. The reduction of I_P by 3.12% also lowers the I_L by 0.06 (from -0.29 to -0.35), which in turn leads to the rise of the undrained shear strength to 321 kPa (Fig.6.5.).

6.5 The undrained shear strength proposed by other authors

Considering properties of the clay till at Simrishamn and Stångby, estimations of undrained shear strength proposed by Wroth and Wood (1978), Luke (1996) and Young and Daehyeon (2011) were applied (see subchapter 2.2) and compared to the obtained undrained shear strength values from this study (Tab. 6.1 and Fig. 6.8). While Wroth and Wood (1978) proposed an estimation of undrained shear strength using the liquidity index and a mathematical constant, Luke (1996) and Young and Daehyeon (2011) suggested a multi-step alternative. First, estimate the cone factor (N_{kt}) employing the friction ratio (R_f) and then the plasticity index (I_P). Afterwards, the undrained shear strength is estimated from CPT measurements by applying the calculated cone factor values.

The analysis shows that the suggested undrained shear strength estimations generally capture the trend. However, it is clearly seen that the shear strength values proposed by Wroth and Wood (1978) and Young and Daehyeon (2011) are underestimated in the brittle and medium soft consistency zones (the purple and gray frames in Fig. 6.8.) and overestimated in the very brittle consistency zone (the red frame in Fig. 6.8).

Table 6.1. A summary of the different undrained shear strength values and related data.

ID	Liquidity index, IL	Plasticity index, IP, %	Natural water content, *w*, %	Total cone resistance, *qt*, kPa	Effective vertical stress, *σv0*	Net tip resistance *(qt-σv0)*	*cuVST*	*cuCPT* in Sweden	*cuCPT* Young and Daehyeon(2011)	*cuCPT* Luke (1996)	*cu* Wroth and Wood, (1978)
								Nkt=11	*Nkt*=0,285*IP+7,636	*Nkt*=15*R f^(-0,4)	*cu*=170*e*^(-4,6*IL)
17T01	-0.35	2.79	13.69	8443	51	8392	-	763	995	544	850.48
	0.12	13.86	19.62	2854	128	2726	-	248	235	227	97.89
17T02	0.23	14.40	22.14	2000	29	1971	-	179	168	208	59.02
	-0.21	5.50	18.85	3352	40	3312	-	301	360	356	446.66
	-0.07	11.51	19.82	2729	49	2680	-	224	245	283	234.58
	0.05	25.10	24.40	2622	120	2502	-	227	169	299	135.07
17T04	-0.29	5.91	12.16	2729	48	2681	-	444	288	548	645.35
	-0.05	6.80	23.10	2622	84	2538	-	313	265	388	213.96
M1719	0.29	5.10	16.20	1251	22	1229	42	112	135	128	43.94
M1716	-0.10	10.61	12.20	2313	24	2289	208	208	215	213	273.86
A1768	0.24	17.82	18.90	910	15	895	93	81	70	105	56.04
	0.24	17.82	18.90	919	22	897	115	82	71	86	56.04
1709	0.29	20.43	18.00	1225	15	1210	100	110	90	-	44.04
	0.26	18.58	19.60	651	24	627	137	57	48	-	51.80
M1701	0.34	17.42	20.60	1093	24	1069	186	97	85	142	34.85
1703	0.25	21.63	17.60	2124	37	2087	101	190	151	225	52.77
1704	0.14	19.35	17.70	2832	15	2817	105	256	214	282	89.47
	0.21	19.90	19.30	808	26	782	135	71	59	101	64.38
1712	0.21	13.50	16.70	1193	26	1167	169	106	102	145	63.27

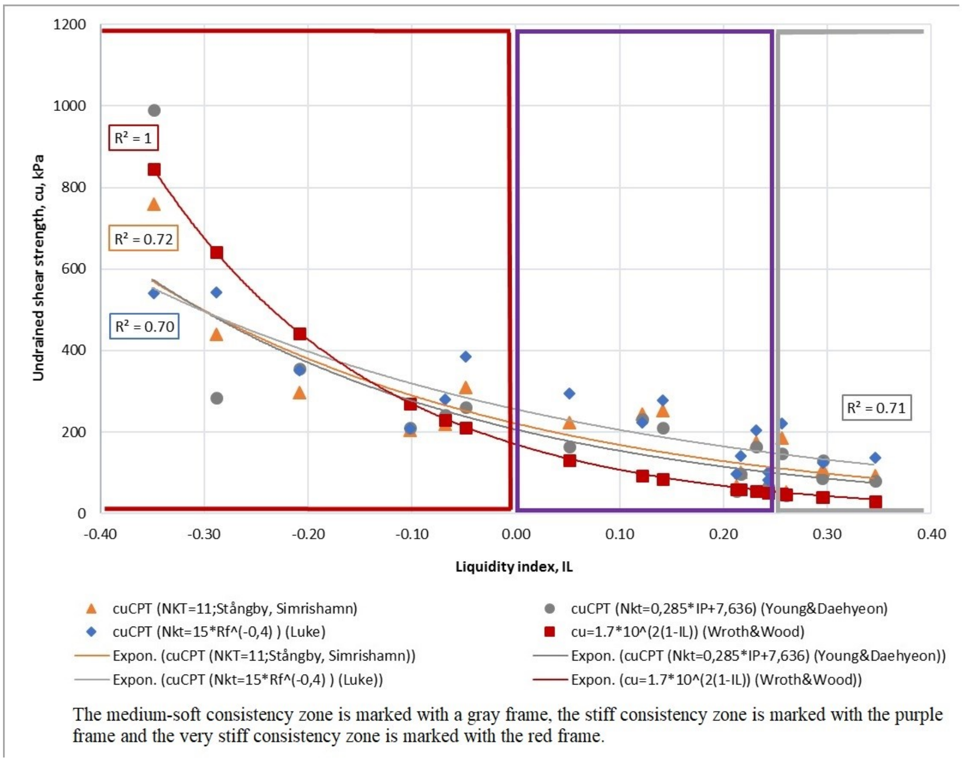

Figure 6.8. A correlation between undrained shear strength and liquidity index from various authors and the results obtained in this study, expressed with exponential regression lines.

The proposed estimation of Luke and the obtained undrained shear strength in this study display principally similar values, albeit even here indicating a small difference of undrained shear strength in the brittle consistency zone, where c_u varies within 4 to 45 kPa range. Additionally, a larger contrast is observed in the very brittle consistency zone where c_u varies within 5 to 219 kPa range. Despite the divergence in the two consistency zones, the correlation between liquidity index and shear strength shows a quite high fit with the three proposed estimations, with R^2= 0.70 for Luke (1996), 0.71 for Young and Daehyeon (2011), and 0.72 for measurements obtained in this study (Fig 6.8).

6.6 Geological aspects

The clay-rich till at the Stångby site, also called Lund Till, was deposited by the Öresund re-advance of the Young Baltic Ice stream at ca 17 kyr BP (Ringberg, 2003; Anjar, 2013). It has a clay content of >25% and a brittle to medium-soft consistency (Tab. 2.2, Fig. 3.5. and 6.9). The characteristic Palaeogene chalk content representing the bedrock of the Baltic Sea was observed in clay till samples (Fig. 3.6).

The plasticity index characterises the plasticity of the sediments, while the liquid limit is the moisture content at which clay-rich sediments change consistency state. The good relation between the liquid limit and the plasticity index found by Dueck (1995) for the Lund Till at Tornhill, was also observed in this study at the Stångby site. Therefore, it indicates that the plasticity of the clay till depends on both the natural water content and the clay content. Unfortunately, the narrow liquidity index range made it impossible to correlate it with the undrained shear strength, as the variations in grain size are crucial for the correlation of these properties.

It is believed that two clay tills were found at the Simrishamn site: a lower, clay-rich, grey till with occasional small rounded Palaeozoic limestone clasts and a clay content of >25%, and an upper, sandy, silty brown clay till with a clay content between 15 and 25% (Fig. 3.5 and 6.9). Considering that the bedrock near Simrishamn and at the bottom of the Baltic Sea consist of shale, sandstone and Palaeozoic limestone

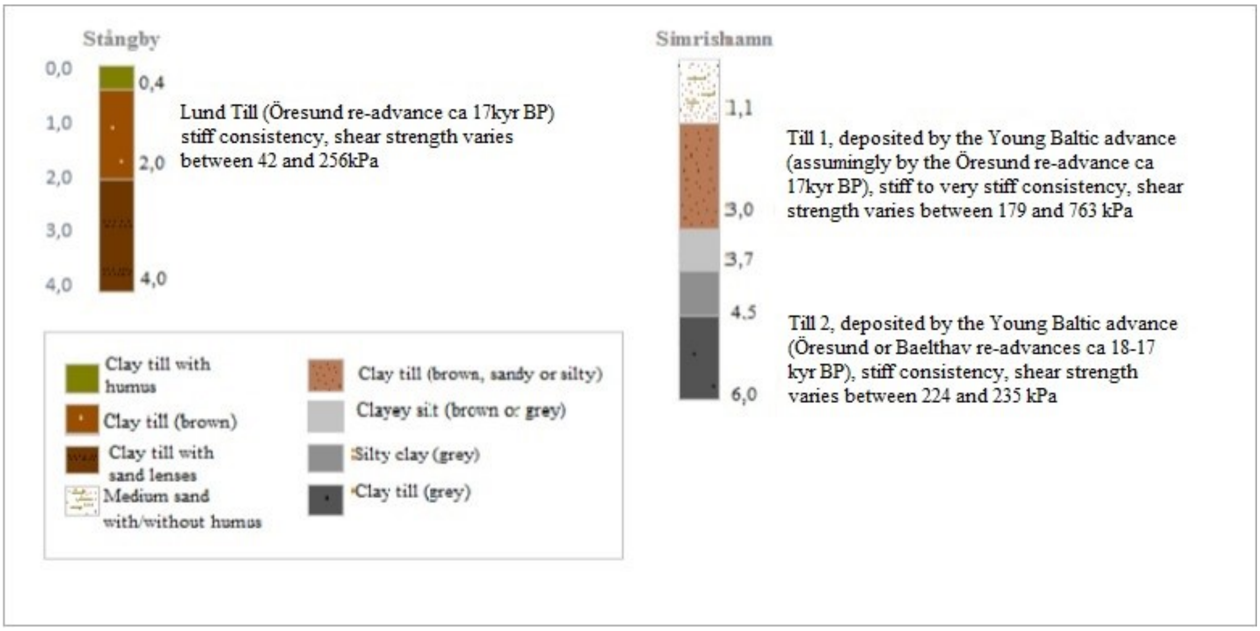

Figure 6.9. Approximate geological cross-section in Stångby and Simrishamn.

(Fredén,1994) it is likely that both tills found at Simrishamn, originated from the Baltic ice advance. However it is assumed that the lowermost grey till might also be deposited by the Bælthav re-advance and the upper by the Öresund re-advance.

Dueck's observed correlation between the liquid limit and the plasticity index for the Lund till at the Tornhill was also found for the assumed two tills at the Simrishamn. The large variation of the grain size in clay tills provided the wide range of liquid and plastic limits as clay particles have large specific area which retain the water. This, in turn, provided a pronounced correlation between the liquidity index and the undrained shear strength. Considering all given information, it is clearly seen that the grain size distribution of the clay till is the main crucial property, which is the prerequisite for the correlation of liquidity index and undrained shear strength.

In conclusion, clay tills in Scania can be categorized in two ways: by the percentage of clay or by the characteristic clasts incorporated in the tills. The analysis in laboratory, CPT and VST shows that the homogeneous Lund Till was deposited at Stångby, possibly two different tills were deposited at Simrishamn. The wide range of grain size in these two tills provided the wide range of liquidity indices and shear strength values. Although all three tills were deposited by the Baltic Ice advance, the grain size distribution and mineralogy varies significantly between them, suggesting that undrained shear strength from liquidity index should be estimated locally.

7 Conclusions

The undrained shear strength is one of the critical strength parameters of a sediments, which is commonly used to analyse stability and lateral pressure at the different stages of the construction projects. Most part of the undrained shear strength tests are cost- and time consuming, thus it is of interest to test the potential relationship with shear strength obtained by different methods by applying alternative, easily measurable parameters such as the liquidity index.

The relationship between the liquidity index and the undrained shear strength in this study was found only partially, as several factors affect these parameters. The liquidity index or consistency of clay tills at the Stångby and Simrishamn sites scatter between 0.44 and 0.58. It is primarily dependent on the composition of the sediments (plasticity index) and less on the natural water content. The study showed that the wide range of the consistency is crucial for the correlation between I_L and c_u.

The undrained shear strength of the clay till is influenced by the granulometric composition, the state of consolidation, the texture, depositional conditions and post-sedimentation changes.

The undrained shear strength from both CPT and VST at Stångby scatter within 199 and 166 kPa range, suggesting that the different methods give different shear strength values and CPT is more susceptible to the inhomogeneities.

While no correlation between the liquidity index and the undrained shear strength was found at Stångby, results from Simrishamn show a quite good correlation (R^2=0.76), suggesting that it is possible to estimate the undrained shear strength from the liquidity index if at least two consistency zones are tested.

8 Proposed further research

This study has provided evidence that the undrained shear strength can be estimated from the liquidity index and that the plasticity of the clay till is a significant property in this relation. The plasticity depends not only on the amount of clay, but also on the type of clay minerals present in the sediments, as the different clay minerals of the clay fraction (2µm) yield the different activity (Skempton, 1984; Dolinar, 2010). Although clay till samples taken from this limited area will presumably show only variations in the percentage of clay, it would be of interest to analyse to what extent various clay minerals of different origin affect the mechanical properties.

Several difficulties should be considered when performing related studies. Firstly, it was found highly complicated to carry out the fall cone test for sandy clay till samples, as the mineral grains were large enough to decelerate the cone from the immersion in the clay till mixture. Therefore, values of liquid limit obtained from sandy clay till might not be highly correct. Secondly, based on the sensitivity of the method to sediment impurities different shear strength methods give different values. Therefore, it is suggested to consider applying only one shear strength method.

9 Acknowledgements

The project was conducted in collaboration with the division of Geotechnical Engineering at the Faculty of Engineering LTH, and the consultancy company Tyréns in Malmö.

My deepest thanks to my supervisors Erika Tudisco and co-supervisor Ola Dahlblom from LTH, who guided me through the geotechnical parts of the thesis. I am grateful to my supervisor, Dan Hammarlund for the inspiration. To my friend, Tove Hernnäs, who went with me to the field and helped to drill and take samples, thank you so much! Also Victor Myrström and Jonas Åkerman from Tyréns made valuable contributions to my thesis, clarifying calculations and discussing results of various laboratory tests. I am grateful Mats Svensson for believing in me. I also want to thank my family for the greatest patience and support and Karina Antonenko, Kyle Bruce, Johan Striberger and Anica Mercado for comments on my manuscript.

10 References

Aas G., Lacasse S., Lunne T., Hoeg K., 1986. Use of in situ tests for foundation design on clay. Proceeding of In Situ'86: Use of In Situ Tests in Geotechnical Engineering, Virginia, pp. 1-30.

Anjar J., 2013. The Weichselian in southern Sweden and southwestern Baltic Sea: glacial stratigraphy palaeoenvironment and deglaciation chronology Doctoral dissertation, Department of Geology, Lund University.

Anjar J., Larsen N.K., Håkansson L., Möller P., Linge H., Fabel D., Xu S., 2014. A ^{10}Be-based reconstruction of the last deglaciation in southern Sweden. Boreas, 43,132-148.

Berglund B.E., Lagerlund E. 1981. Eemian and Weichselian stratigraphy in South Sweden. Boreas 10, 323-362.

Bjerrum L., 1954. Geotechnical properties of Norwegian marine clays. Géotechnique, 4: 49-69.

Bjerrum L., 1973. Problems of soil mechanics and construction on soft clays and structurally unstable soils (collapsible, expansive and others). In: Proceedings of the 8th International Conference on Soil Mechanics and Foundation Engineering, Moscow; 111-59.

Daniel E., 1986. Description of the Quaternary maps Tomelilla SO/Simrishamn SV Ystad NO/ Örnahusen NV; the geological Survey of Sweden SGU, Uppsala, Sweden Offset center AB

Daniel E., Malmberg Persson K. & Persson M., 2000: Quaternary deposits of Scania, 1:250 000. Sveriges Geologiska Undersökning Ba 55.

Dansk Geoteknisk Forening Feltkomité, 1998. Referensblad for vingeforsøg. Referenceblad 1, revision 3. Dansk Geoteknisk Forening, København

Dolinar B., 2010. Predicting the normalized, undrained shear strength of saturated fine-grained soils using plasticity-value corrections. Applied Clay Science, 47 (3-4): 428-432.

Dueck A., 1995. Reference Site for Clay Till. Lund Institute of Technology, Lund University, Department of Geotechnology, LUTVDG/TVGT-3025-SE

Dueck A., 1997. Egenskaper i lermorän. En laboratoriestudie utförd vid Laboratoriet for Fundering, Aalborgs Universitetscenter. Institute of Technology, Lund University, Department of Geotechnology, LUTVDG/TVGT – 3028-SE

Dueck A., 1998. Shear strength and matric suction in clay tills- Triaxial test procedure to evaluate shear strength of clay tills from south-western Sweden. Lunds Tekniska Högskola, Avdelning för Geoteknik, Lund, Sweden, KFS AB Lund

Duncan J.M., Wright S.G., Brandon T.L., 2014. Soil Strength and Slope Stability. Second Edition, John Wiley&Sons, Inc., New Jersey, USA and Canada.

Ekström G., 1936. Skånes moränområden. Svensk Geografisk Årsbok 12: 70–77

Ekström G., 1950. Skånes åkerjordsområden. Socker, Handlingar Årg. 6.

Fredén C., 1994. National Atlas of Sweden. Geology. first edition, Italy.

Hartlén J., 1974. Skånska moränlerors hållfasthets och bärighetsegenskaper. Dr. Thesis; Chalmers University of Technology; Göteborg, Sweden.

Jacobsen M. 1970. Strength and Deformation Properties of Preconsolidated Moraine Clay. In Bulletin No 27: 21-45. Kbh: The Danish Geotechnical Institute.

Karpovics A., 2010. Glacigenic soil geotechnical properties and their variability in Latvia. Faculty of Geography and Earth Sciences, Latvian University

Kayabali K., Akturk O., Fener M., Dikmen O., Harputlugil F.H., 2015. Revisiting the Bjerrum's correction factor: Use of the liquidity index for assessing the effect of soil plasticity on undrained shear strength. Journal of Rock Mechanics and Geotechnical Engineering, 7,716-721.

Knappett J.A., Craig R.F., 2012. Craig's Soil Mechanics, Eighth edition, Canada and USA, Spon Press.

Larsson R., 2001. Investigation and Load Tests in Clay Till. Results from a series of investigation and load tests in the test field at Tornhill outside Lund in southern Sweden. Swedish Geotechnical Institute. Linköping, Sweden.

Larsson R., Sällfors G., Bengtsson P.E., Alén C., Eriksson L., 2007. Skjuvhållfasthet-utvärdering i kohesionsjord. Andra utgåvan- reviderad, Statens Geotekniska Institut, Linköping, Sweden.

Larsson R., 2008. Jords egenskaper. 5:e utgåvan-reviderad, Statens Geotekniska Institut, Linköping, Sweden.

Larsson R., 2015. CPT-sondering, Utrustning-Utförande-Utvärdering. En in-situ metod för bestämning av jordlagerföljd och egenskaper i jord. Tredje utgåvan-reviderad. Statens Geotekniska Institut, Linköping, Sweden.

Leroueil S., Tavenas F., and Bihan J.L., 1983. Propriétés caractéristiques des argiles de l'est du Canada. Canadian Geotechnical Journal, 20(4): 681-705. (In French)

Locat J., and Damers D., 1988. Viscosity, yield stress, remolded strength, and liquidity index relationships for sensitive clays. Canadian Geotechnical Journal, 25(4):799-806.

Luke K., 1994. The Use of CPT in Danish Soils – with special Emphasis on Measuring the Undrained Shear Strength. PhD. thesis, Aalborg University

Luke K., 1996. Cone Factors from Field Vane and Triaxial Tests in Danish Soils. In S. Erlingsson, & H. Sigursteinsson (Eds.), Proceedings of the XII Nordic Geotechnical Conference: NGM-96: Reykjavik, 26-28 June 1996 (Vol. 1, 203-208). Icelandic Geotechnical Society.

Lunne T., Eide O., and de Ruiter J. 1976. Correlation between cone resistance and vane shear strength in some Scandinavian soft to medium brittle clays. Canadian Geotechnical Journal, Vol. 13 (4), 430-441.

Mayne P., Coop M., Springman S., Huang A., Zornberg J., 2009. Geomaterial behavior and testing, 17th International Conference in Soil Mechanics and Geotechnical Engineering, In: Proceedings of the 17th International Conference in Soil Mechanics and Geotechnical Engineering, IOS

Press/Millpress Science, 2777-2872.

Mitchell J. K., Soga K. 2005. Fundamentals of Soil Behavior. Third Edition, New Jersey, USA and Canada. John Wiley&Sons, Inc.

Murthy V.N.S., 2002. Geotechnical Engineering: Principles and practices of Soil Mechanics and Foundation Engineering, New York, USA, Marcel Dekker Inc.

Nwobasi P., A., Egba E.I., 2013. Estimation of Undrained Shear Strength of Soil using Cone Penetration Test. International Journal of Scientific & Engineering Research, Volume 4, Issue 9:409-420.

Patton H., Hubbard A., Andreassen K., Auriac A., Whitehouse P.L., Stroeven A.P. Shackleton C., Winsborrow M., Heyman J., Hall A.M., 2017. Deglaciation of the Eurasian ice sheet complex. Quaternary Science reviews Vol.169, 148-172.

Rémai Z., 2012. Correlation of undrained shear strength and CPT resistance. Periodica Polytechnica Civil Engineering 57/1; http://periodicapolytechnica.org/ci; 39-44.

Ringberg B., 2003. Readvance and retreat of the Late Weichselian Low Baltic ice stream in southernmost Sweden – a review. GFF 125, 169 - 176

Ringberg B., 1987. Description of the quaternary map Malmö NO; the geological Survey of Sweden SGU, Uppsala, Sweden Offset center AB

Sandgren P., Snowball I., Hammarlund D., Risberg J., 1999. Stratigraphic evidence for a high marine shoreline during the Late Weichselian deglaciation on the Kullen Peninsula, southern Sweden. Journal of Quaternary Science 14, 223-237.

Skempton A.W., 1984. The Colloidal Activity of Clays. Selected papers on soil mechanics. 60-64

Steenfelt J. S., Sørensen C.S., 1995. CPT- Contraption for probing in Tills? Field Testing Paper R 9517. Aalborg: Geotechnical Engineering Group, Aalborg.

Swedgeo, 2017. Undersökningsmetoder. Available at: http://www.swedgeo.se (accessed 14 March 2018).

Svenska Geotekniska Föreningen, 2013. Geoteknisk Fälthandbok. Version 1.0. SGF Rapport 1:2013, Göteborg, Sweden.

Svenska Geotekniska Föreningen, 2017. Metodik för bestämning av skjuvhållfasthet i lera. En vägledning. SGF Rapport 1:2017, Linköping, Sweden.

Sveriges Geologiska Undersökning, 1980. Jorddjupskarta över Sydvästra Skåne. 1: 100 000, Ser. Ba nr 28, Liber Kartor, Stockholm

Sveriges Geologiska Undersökning, 1985. Jordartskartan. 1:50 000, Ser. Ae nr.65, 2DTomelilla SO/2E Simrishamn SV, Offset Center AB, Uppsala, Sweden

Sveriges Geologiska Undersökning, 1987. Jordartsgeologiska kartblad. 1:50 000, Ser. Ae nr 85, 2C Malmö NO, Offset Center AB, Uppsala, Sweden

Sveriges Geologiska Undersökning, 2017. Jorddjupskarta 1:500 000, SWEREF 99 TM and SWEREF 99, available at http://www.sgu.se (accessed 14 March 2018).

Sveriges Geologiska Undersökning, 2018a, SGU:s kartvisare Jordarter 1:25 000 - 1:100 000, SWEREF 99 TM, available at http://www.sgu.se (assceesed 14 March 2018).

Sveriges Geologiska Undersökning, 2018b, SGU:s kartvisare Jordarter 1:25 000 - 1:100 000, SWEREF 99 TM, available at http://www.sgu.se (accessed 14 January 2018).

Sveriges Nationalatlas, 1999. Atlas över Skåne. Första utgåvan, Uppsala, Sweden, Almqvist & Wiksell

Swedish Standards Institute, 2014. Geotechnical investigation and testing-Laboratory testing of soil-Part 1: Determination of water content (SS EN ISO 17892-1:2014), Edition 1, Brussels.

Swedish Standards Institute, 2008. Geotechnical investigation and testing-Laboratory testing of soils Part 12-Determination of Atterberg limits (ISO/TS 17892-12:2007), Edition 1, Brussels.

Terzaghi K von, 1925. Simplified soil tests for subgrades and their physical significance. Public Roads, 7(8): 155-162, 170

Tyréns, 2017a. MUR (Markteknisk undersökningsrapport) / geoteknik och miljögeoteknik Stångby Väster II. Final rapport. Malmö, Sweden

Tyréns, 2017b MUR (Markteknisk undersökningsrapport) / geoteknik Solrosen 17, Simrishamn. Final rapport,.Malmö Sweden

Venkatramaiah C., 2006. Geotechnical Engineering. New Delhi, India New Age International Publishers.

Wroth C.P., Wood D.M., 1978. The correlation of index properties with some basic engineering properties of soils. Canadian Geotechnical Journal 15(2): 137-145.

Young J.S., Daehyeon K., 2011. Assessment of Undrained Shear Strength based on Cone Penetration Test (CPT) for Clayey Soils KSCE Journal of Civil Engineering 15 (7): 1161-1166.

1 Appendices

Appendix A. *Cone immersion i and M, N values (modified from Larsson), 2008)*

Cone immersion, i, mm (integer)	Value	Cone immersion, mm (tenth)									
		0	1.00	2.00	3.00	4.00	5.00	6.00	7.00	8.00	9.00
7.00	M	1.21	1.2	1.19	1.19	1.19	1.16	1.15	1.14	1.14	1.13
	N	-3.5	-3.4	-3.2	-3	-2.9	-2.7	-2.6	-2.5	-2.3	-2.2
8.00	M	1.12	1.11	1.11	1.1	1.1	1.09	1.08	1.07	1.07	1.06
	N	-2.1	-1.9	-1.8	-1.7	-1.6	-1.4	-1.3	-1.2	-1.1	-1
9.00	M	1.05	1.05	1.04	1.04	1.03	1.03	1.02	1.01	1.01	1
	N	-0.9	-0.8	-0.7	-0.6	-0.5	-0.4	-0.3	-0.3	-0.2	-0.1
10.00	M	1	1	0.99	0.99	0.98	0.98	0.97	0.97	0.96	0.96
	N	0	0.1	0.2	0.2	0.3	0.4	0.5	0.5	0.6	0.7
11.00	M	0.96	0.95	0.95	0.94	0.94	0.94	0.93	0.93	0.93	0.92
	N	0.7	0.8	0.9	0.9	1	1.1	1.1	1.2	1.3	1.3
12.00	M	0.92	0.92	0.91	0.91	0.91	0.9	0.9	0.9	0.89	0.89
	N	1.4	1.4	1.5	1.5	1.6	1.7	1.7	1.8	1.8	1.9
13.00	M	0.89	0.88	0.88	0.88	0.88	0.87	0.87	0.87	0.87	0.86
	N	1.9	2	2	2.1	2.1	2.2	2.2	2.2	2.3	2.3

Appendix B. *Natural water content, liquid limit, plastic limit summary and Vane shear test results from the Stångby site.*

NATURAL WATER CONTENT		Moist weight+ container,g	Dry weight+ container,g	Mass of container ,g	Mass of moist weight, g	Mass of dried weight g	Mass of water,g	ISO/TS 17892-12:2004
ID	Sample depth,							Natural water content, w, %
M1719	1.0-1.5	66.6	57.6	1.9	64.7	55.7	9.00	16.2%
M1716	1.0-1.5	64.4	57.6	1.7	62.7	55.9	6.80	12.2%
A1768	0.3-1.0	44.7	37.9	1.9	42.8	36.0	6.80	18.9%
1709	0.3-1.0	44.0	37.6	2.0	42.0	35.6	6.40	18.0%
1709	1.0-2.2	47.7	40.2	2.0	45.7	38.2	7.50	19.6%
M1701	1.1-1.3	64.9	54.1	1.7	63.2	52.4	10.80	20.6%
1703	1.6-1.8	71.2	60.8	1.8	69.4	59.0	10.40	17.6%
1704	0.6-0.8	64.9	55.4	1.7	63.2	53.7	9.50	17.7%
1704	1.0-1.3	91.4	76.9	1.7	89.7	75.2	14.50	19.3%
1712	1.1-1.3	73.6	63.3	1.8	71.8	61.5	10.30	16.7%

LIQUID LIMIT		Measure ment	Cone immersion 1, mm	Cone immersion 2, mm	Cone immersion 3, mm	Immersion, AVG, mm			Mass of moist weight, g	Mass of dried weight,md, g	Mass of container, g	Mass of water, g	Water content, %	Liquid limit, wL, %	AVG Liquid limit, wL, %
ID	Sample depth,						M value	N value							
M1719	1.0-1.5	I	8.0	9.0	9.0	8.7	1.07	-1.2	48.2	40.7	1.9	7.5	19%	19.5	19.48
M1716	1.0-1.5	I	8.5	10.0	7.0	8.5	1.09	-1.4	60.8	49.7	1.9	11.1	23.2%	23.9	23.91
A1768	0.3-1.0	I	8.0	8.5	8.0	8.2	1.11	-1.8	60.6	46.9	1.9	13.7	30.4%	32.0	32.42
		II	8.0	8.5	10.0	8.8	1.07	-1.1	106.1	81.0	1.9	25.1	31.7%	32.9	
1709	0.3-1.0	I	8.0	7.0	7.0	7.3	1.18	-3.0	46.5	36.2	1.9	10.3	30.0%	32.4	32.43
1709	1.0-2.2	I	14.0	11.0	13.0	12.7	0.90	1.8	52.4	39.6	1.9	12.8	34.0%	32.4	33.38
		II	12.0	14.0	13.0	13.0	0.89	1.9	43.5	33.1	1.9	10.4	33.3%	31.6	
		III	11.0	13.0	12.0	12.0	0.92	1.4	32.5	24.1	1.9	8.4	37.8%	36.2	
M1701	1.1-1.3	I	12.0	12.0	10.0	11.3	0.94	0.9	67.4	51.1	1.9	16.3	33.1%	32.0	32.02
		II	13.0	13.0	13.0	13.0	0.89	1.9	49.0	37.1	1.9	11.9	33.8%	32.0	
1703	1.6-1.8	I	13.0	12.0	13.0	12.7	0.90	1.8	71.0	53.2	1.9	17.8	34.7%	33.0	33.73
		II	12.0	13.0	13.0	12.7	0.90	1.8	47.0	35.0	1.9	12.0	36.3%	34.4	
1704	0.6-0.8	I	13.0	10.0	13.0	12.0	0.92	1.4	87.4	65.1	1.9	22.3	35.3%	33.9	34.35
		II	11.0	10.0	12.0	11.0	0.96	0.7	44.6	33.4	1.9	11.2	35.6%	34.8	
1704	1.0-1.3	I	12.5	11.0	13.0	12.2	0.91	1.5	58.3	43.2	1.9	15.1	36.6%	34.8	35.00
		II	12.0	9.0	12.0	11.0	0.96	0.7	60.5	45.0	1.9	15.5	36.0%	35.2	
1712	1.1-1.3	I	10.0	10.0	8.5	9.5	1.03	-0.4	63.4	50.4	1.9	13.0	26.8%	27.2	27.30
		II	7.5	8.5	10.0	8.7	1.07	-1.2	53.6	42.7	1.9	10.9	26.7%	27.4	

ISO/TS 17892-12:2004 PLASTIC LIMIT		Moist weight+ container, g	Dry weight+ container, g	Mass of container, g	Mass of moist weight, g	Mass of dried weight, g	Mass of water, g	Plastic limit, wp, %
ID	Sample depth, m							
M1719	1.0-1.5	9.8	8.8	2.0	7.8	6.8	1.0	14.7%
M1716	1.0-1.5	10.5	9.5	2.0	8.5	7.5	1.0	13.3%
A1768	0.3-1.0	11.4	10.2	2.0	9.4	8.2	1.2	14.6%
1709	0.3-1.0	7.6	7.0	2.0	5.6	5.0	0.6	12.0%
1709	1.0-2.0	8.2	7.4	2.0	6.2	5.4	0.8	14.8%
M1701	1.1-1.3	31.5	27.7	1.7	29.8	26.0	3.8	14.6%
1703	1.6-1.8	36.9	33.1	1.8	35.1	31.3	3.8	12.1%
1704	0.6-0.8	38.6	33.8	1.9	36.7	31.9	4.8	15.0%
1704	1.0-1.3	41.4	36.2	1.8	39.6	34.4	5.2	15.1%
1712	1.1-1.3	38.9	34.4	1.7	37.2	32.7	4.5	13.8%

SUMMARY					Ip=wL-wp	IL=w-wp/wL-wp
ID	Sample depth, m	Water content,w	Liquid limit, wL,	Plastic limit, wp,	Plasticity Index, Ip, %	Liquidity index, IL, %
M1719	1.0-1.5	16.20	19.80	14.70	5.10	0.29
M1716	1.0-1.5	12.20	23.91	13.30	10.61	- 0.10
A1768	0.3-1.0	18.90	32.42	14.60	17.82	0.24
1709	0.3-1.0	18.00	32.43	12.00	20.43	0.29
1709	1.0-2.0	19.60	33.38	14.80	18.58	0.26
M1701	1.1-1.3	20.60	32.02	14.60	17.42	0.34
1703	1.6-1.8	17.60	33.73	12.10	21.63	0.25
1704	0.6-0.8	17.70	34.35	15.00	19.35	0.14
1704	1.0-1.3	19.30	35.00	15.10	19.90	0.21
1712	1.1-1.3	16.70	27.30	13.80	13.50	0.21

Vane Shear Test			Momentum, *Nm*		
ID	Sample depth, m	Depth, m		Cu, *Pa*	Cu, *Kpa*
M1719	1.0-1.5	1.0	17.0	41503.9	42
M1716	1.0-1.5	1.1	85.0	207519.5	208
A1768	0.3-1.0	0.7	38.0	92773.4	93
A1768	0.3-1.0	1.0	47.0	114746.1	115
1709	0.3-1.0	0.7	41.0	100097.7	100
1709	1.0-2.0	1.1	56.0	136718.8	137
M1701	1.1-1.3	1.1	76.3	186279.3	186
M1701	1.1-1.3	1.5	78.2	190918.0	191
1703	1.6-1.8	1.7	41.2	100585.9	101
1704	0.6-0.8	0.7	43.0	104980.5	105
1704	1.0-1.3	1.2	55.3	135009.8	135
1707	1.1-1.3	1.2	33.7	82275.4	82
1712	1.1-1.3	1.2	69.3	169189.5	169

Appendix C. *CPT results from Stångby*

ID	Disturbed Sample depth, m	CPT depth, m	Unit weight, γ, kN/m3	Effective vertical stress, kPa	Total cone tip resistance, qc, MPa	Total cone tip resistance, qc, kPa	AVG cone tip resistence, qc, kPa	Pore pressure *u*, *kPa*	a factor	1-a	Total cone resistance, qt, kPa	Cone factor, Nkt	Shear strength, cu, kPa	Liquidity index, IL
M1719	1.0 -1.5	0.96	22	21.1	1.29	1290		117.0	0.849	0.151	1307.67	11	117	0.29
		0.98	22	21.6	1.23	1230	1260	187.7	0.849	0.151	1258.34	11	112	
		1.00	22	22.0	1.23	1230	1230	142.5	0.849	0.151	1251.52	11	112	
		1.02	22	22.4	1.24	1240	1235	93.9	0.849	0.151	1254.18	11	112	
		1.04	22	22.9	1.20	1200	1220	176.0	0.849	0.151	1226.58	11	109	
		1.06	22	23.3	1.19	1190	1195	225.0	0.849	0.151	1223.98	11	109	
		1.08	22	23.8	1.27	1270	1230	223.0	0.849	0.151	1303.67	11	116	
		1.10	22	24.2	1.26	1260	1265	200.5	0.849	0.151	1290.28	11	115	
		1.12	22	24.6	1.18	1180	1220	219.8	0.849	0.151	1213.19	11	108	
		1.14	22	25.1	1.12	1120	1150	212.6	0.849	0.151	1152.10	11	102	
		1.16	22	25.5	1.07	1070	1095	255.4	0.849	0.151	1108.57	11	98	
		1.18	22	26.0	1.06	1060	1065	280.8	0.849	0.151	1102.40	11	98	
		1.20	22	26.4	1.08	1080	1070	351.6	0.849	0.151	1133.09	11	101	
		1.22	22	26.8	1.35	1350	1215	364.3	0.849	0.151	1405.01	11	125	
		1.24	22	27.3	1.49	1490	1420	312.0	0.849	0.151	1537.11	11	137	
		1.26	22	27.7	1.58	1580	1535	366.1	0.849	0.151	1635.28	11	146	
		1.28	22	28.2	1.66	1660	1620	385.2	0.849	0.151	1718.17	11	154	
		1.30	22	28.6	1.74	1740	1700	400.1	0.849	0.151	1800.42	11	161	
		1.32	22	29.0	1.77	1770	1755	337.8	0.849	0.151	1821.01	11	163	
		1.34	22	29.5	1.91	1910	1840	479.9	0.849	0.151	1982.46	11	178	
		1.36	22	29.9	2.21	2210	2060	523.4	0.849	0.151	2289.03	11	205	
		1.38	22	30.4	2.45	2450	2330	262.5	0.849	0.151	2489.64	11	224	
		1.40	22	30.8	2.15	2150	2300	269.3	0.849	0.151	2190.66	11	196	
		1.42	22	31.2	2.03	2030	2090	338.1	0.849	0.151	2081.05	11	186	
		1.44	22	31.7	1.76	1760	1895	465.2	0.849	0.151	1830.25	11	164	
		1.46	22	32.1	1.82	1820	1790	594.0	0.849	0.151	1909.69	11	171	
		1.48	22	32.6	1.93	1930	1875	695.3	0.849	0.151	2034.99	11	182	
		1.50	22	33.0	2.02	2020	1975	767.2	0.849	0.151	2135.85	11	191	

ID	Disturbed Sample depth, m	CPT depth, m	Unit weight, γ, kN/m3	Effective vertical stress, kPa	Total cone tip resistance, qc, MPa	Total cone tip resistance, qc, kPa	AVG cone tip resistence, qc, kPa	Pore pressure *u*, *kPa*	a factor	1-a	Total cone resistance, qt, kPa	Cone factor, Nkt	Shear strength, cu, kPa	Liquidity index, IL
1716	1.0 -1.5	1.00	22	22.0	2.13	2130		315.0	0.849	0.151	2177.57	11	196	-0.1
		1.02	22	22.4	2.09	2090	2110	390.6	0.849	0.151	2148.98	11	193	
		1.04	22	22.9	2.08	2080	2085	484.2	0.849	0.151	2153.11	11	194	
		1.06	22	23.3	2.13	2130	2105	524.5	0.849	0.151	2209.20	11	199	
		1.08	22	23.8	2.17	2170	2150	492.1	0.849	0.151	2244.31	11	202	
		1.10	22	24.2	2.24	2240	2205	487.9	0.849	0.151	2313.67	11	208	
		1.12	22	24.6	2.40	2400	2320	443.8	0.849	0.151	2467.01	11	222	
		1.14	22	25.1	2.32	2320	2360	471.1	0.849	0.151	2391.14	11	215	
		1.16	22	25.5	2.32	2320	2320	519.6	0.849	0.151	2398.46	11	216	
		1.18	22	26.0	2.26	2260	2290	500.9	0.849	0.151	2335.64	11	210	
		1.20	22	26.4	2.22	2220	2240	597.5	0.849	0.151	2310.22	11	208	
		1.22	22	26.8	2.29	2290	2255	657.6	0.849	0.151	2389.30	11	215	
		1.24	22	27.3	2.31	2310	2300	604.3	0.849	0.151	2401.25	11	216	
		1.26	22	27.7	2.32	2320	2315	685.3	0.849	0.151	2423.48	11	218	
		1.28	22	28.2	2.42	2420	2370	654.3	0.849	0.151	2518.80	11	226	
		1.30	22	28.6	2.37	2370	2395	640.4	0.849	0.151	2466.70	11	222	
		1.32	22	29.0	2.29	2290	2330	628.7	0.849	0.151	2384.93	11	214	
		1.34	22	29.5	2.23	2230	2260	769.7	0.849	0.151	2346.22	11	211	
		1.36	22	29.9	2.22	2220	2225	745.7	0.849	0.151	2332.60	11	209	
		1.38	22	30.4	2.23	2230	2225	704.7	0.849	0.151	2336.41	11	210	
		1.40	22	30.8	2.21	2210	2220	741.3	0.849	0.151	2321.94	11	208	
		1.42	22	31.2	2.25	2250	2230	759.9	0.849	0.151	2364.74	11	212	
		1.44	22	31.7	2.26	2260	2255	828.7	0.849	0.151	2385.13	11	214	
		1.46	22	32.1	2.31	2310	2285	839.6	0.849	0.151	2436.78	11	219	
		1.48	22	32.6	2.37	2370	2340	877.4	0.849	0.151	2502.49	11	225	
		1.50	22	33.0	2.44	2440	2405	861.5	0.849	0.151	2570.09	11	231	

ID	Disturbed Sample depth, m	CPT depth, m	Unit weight, γ, kN/m3	Effective vertical stress, kPa	Total cone tip resistance, qc, MPa	Total cone tip resistance, qc, kPa	AVG cone tip resistence, qc, kPa	Pore pressure *u*, *kPa*	a factor	1-a	Total cone resistance, qt, kPa	Cone factor, Nkt	Shear strength, cu, kPa	Liquidity index, IL
1704	0.6-0.8	0.60	22	13.2	1.25	1250		9.8	0.823	0.177	1252	11	113	0.14
		0.62	22	13.6	2.44	2440	1845	12.6	0.823	0.177	2442	11	221	
		0.64	22	14.1	3.13	3130	2785	-21.3	0.823	0.177	3126	11	283	
		0.66	22	14.5	2.58	2580	2855	86.0	0.823	0.177	2595	11	235	
		0.68	22	15.0	4.33	4330	3455	76.2	0.823	0.177	4343	11	394	
		0.70	22	15.4	2.82	2820	3575	68.1	0.823	0.177	2832	11	256	
		0.72	22	15.8	2.82	2820	2820	35.8	0.823	0.177	2826	11	255	
		0.74	22	16.3	2.82	2820	2820	43.0	0.823	0.177	2828	11	256	
		0.76	22	16.7	3.14	3140	2980	28.5	0.823	0.177	3145	11	284	
		0.78	22	17.2	1.86	1860	2500	22.2	0.823	0.177	1864	11	168	
		0.80	22	17.6	1.86	1860	1860	32.5	0.823	0.177	1866	11	168	
1704	1.0-1.3	1.00	22	22.0	0.99	990		79.9	0.823	0.177	1004	11	89	0.21
		1.02	22	22.4	1.10	1100	1045	87.0	0.823	0.177	1115	11	99	
		1.04	22	22.9	1.25	1250	1175	83.5	0.823	0.177	1265	11	113	
		1.06	22	23.3	0.90	900	1075	111.3	0.823	0.177	920	11	81	
		1.08	22	23.8	0.92	920	910	125.8	0.823	0.177	942	11	84	
		1.10	22	24.2	0.92	920	920	131.6	0.823	0.177	943	11	84	
		1.12	22	24.6	0.93	930	925	86.3	0.823	0.177	945	11	84	
		1.14	22	25.1	0.84	840	885	88.1	0.823	0.177	856	11	76	
		1.16	22	25.5	0.81	810	825	89.3	0.823	0.177	826	11	73	
		1.18	22	26.0	0.81	810	810	94.2	0.823	0.177	827	11	73	
		1.20	22	26.4	0.79	790	800	102.1	0.823	0.177	808	11	71	
		1.22	22	26.8	0.75	750	770	101.9	0.823	0.177	768	11	67	
		1.24	22	27.3	0.76	760	755	101.5	0.823	0.177	778	11	68	
		1.26	22	27.7	0.89	890	825	103.0	0.823	0.177	908	11	80	
		1.28	22	28.2	0.89	890	890	109.9	0.823	0.177	909	11	80	
		1.30	22	28.6	1.07	1070	980	117.7	0.823	0.177	1091	11	97	

ID	Disturbed Sample depth, m	CPT depth, m	Unit weight, γ, kN/m3	Effective vertical stress, kPa	Total cone tip resistance, qc, MPa	Total cone tip resistance, qc, kPa	AVG cone tip resistence, qc, kPa	Pore pressure *u*, *kPa*	a factor	1-a	Total cone resistance, qt, kPa	Cone factor, Nkt	Shear strength, cu, kPa	Liquidity index, IL
1712	1.0 -1.3	1.00	22	22.0	1.25	1250		102.6	0.823	0.177	1268.1602	11	113	0.21
		1.02	22	22.4	1.25	1250	1250	111	0.823	0.177	1269.647	11	113	
		1.04	22	22.9	1.21	1210	1230	104.6	0.823	0.177	1228.5142	11	110	
		1.06	22	23.3	1.24	1240	1225	111.9	0.823	0.177	1259.8063	11	112	
		1.08	22	23.8	1.21	1210	1225	128.7	0.823	0.177	1232.7799	11	110	
		1.10	22	24.2	1.17	1170	1190	160.4	0.823	0.177	1198.3908	11	107	
		1.12	22	24.6	1.13	1130	1150	155.1	0.823	0.177	1157.4527	11	103	
		1.14	22	25.1	1.13	1130	1130	169.2	0.823	0.177	1159.9484	11	103	
		1.16	22	25.5	1.14	1140	1135	156.3	0.823	0.177	1167.6651	11	104	
		1.18	22	26.0	1.16	1160	1150	168.2	0.823	0.177	1189.7714	11	106	
		1.20	22	26.4	1.16	1160	1160	189.9	0.823	0.177	1193.6123	11	106	
		1.22	22	26.8	1.16	1160	1160	201.5	0.823	0.177	1195.6655	11	106	
		1.24	22	27.3	1.21	1210	1185	195.1	0.823	0.177	1244.5327	11	111	
		1.26	22	27.7	1.31	1310	1260	194.3	0.823	0.177	1344.3911	11	120	
		1.28	22	28.2	1.31	1310	1310	191.5	0.823	0.177	1343.8955	11	120	
		1.30	22	28.6	1.41	1410	1360	157.5	0.823	0.177	1437.8775	11	128	

ID	Disturbed Sample depth, m	CPT depth, m	Unit weight, γ, kN/m3	Effective vertical stress, kPa	Total cone tip resistance, qc, MPa	Total cone tip resistance, qc, kPa	AVG cone tip resistence, qc, kPa	Pore pressure *u*, *kPa*	a factor	1-a	Total cone resistance, qt, kPa	Cone factor, Nkt	Shear strength, cu, kPa	Liquidity index, IL
1709	0.3-1.0	0.30	22	6.6	0.83	830		-7.4	0.849	0.151	828.8826	11	75	0.29
		0.32	22	7.0	0.85	850	840	-10.2	0.849	0.151	848.4598	11	76	
		0.34	22	7.5	0.88	880	865	-14.8	0.849	0.151	877.7652	11	79	
		0.36	22	7.9	0.89	890	885	-8.4	0.849	0.151	888.7316	11	80	
		0.38	22	8.4	0.93	930	910	-7.4	0.849	0.151	928.8826	11	84	
		0.40	22	8.8	0.96	960	945	-5.5	0.849	0.151	959.1695	11	86	
		0.42	22	9.2	1.00	1000	980	-6.0	0.849	0.151	999.094	11	90	
		0.44	22	9.7	1.09	1090	1045	-6.1	0.849	0.151	1089.0789	11	98	
		0.46	22	10.1	1.14	1140	1115	-0.6	0.849	0.151	1139.9094	11	103	
		0.48	22	10.6	1.20	1200	1170	2.1	0.849	0.151	1200.3171	11	108	
		0.50	22	11.0	1.26	1260	1230	1.8	0.849	0.151	1260.2718	11	114	
		0.52	22	11.4	1.26	1260	1260	6.3	0.849	0.151	1260.9513	11	114	
		0.54	22	11.9	1.23	1230	1245	1.9	0.849	0.151	1230.2869	11	111	
		0.56	22	12.3	1.14	1140	1185	-2.1	0.849	0.151	1139.6829	11	102	
		0.58	22	12.8	1.10	1100	1120	1.8	0.849	0.151	1100.2718	11	99	
		0.60	22	13.2	1.09	1090	1095	15.3	0.849	0.151	1092.3103	11	98	
		0.62	22	13.6	1.09	1090	1090	40.2	0.849	0.151	1096.0702	11	98	
		0.64	22	14.1	1.08	1080	1085	38.2	0.849	0.151	1085.7682	11	97	
		0.66	22	14.5	1.12	1120	1100	27.0	0.849	0.151	1124.077	11	101	
		0.68	22	15.0	1.17	1170	1145	30.7	0.849	0.151	1174.6357	11	105	
		0.70	22	15.4	1.22	1220	1195	38.3	0.849	0.151	1225.7833	11	110	
		0.72	22	15.8	1.21	1210	1215	18.9	0.849	0.151	1212.8539	11	109	
		0.74	22	16.3	1.18	1180	1195	30.0	0.849	0.151	1184.53	11	106	
		0.76	22	16.7	1.16	1160	1170	15.6	0.849	0.151	1162.3556	11	104	
		0.78	22	17.2	1.11	1110	1135	18.8	0.849	0.151	1112.8388	11	100	
		0.80	22	17.6	1.08	1080	1095	6.1	0.849	0.151	1080.9211	11	97	
		0.82	22	18.0	1.01	1010	1045	-5.5	0.849	0.151	1009.1695	11	90	
		0.84	22	18.5	0.95	950	980	-8.7	0.849	0.151	948.6863	11	85	
		0.86	22	18.9	0.91	910	930	4.5	0.849	0.151	910.6795	11	81	
		0.88	22	19.4	0.89	890	900	-3.7	0.849	0.151	889.4413	11	79	
		0.90	22	19.8	0.86	860	875	-4.8	0.849	0.151	859.2752	11	76	
		0.92	22	20.2	0.81	810	835	3.7	0.849	0.151	810.5587	11	72	
		0.94	22	20.7	0.82	820	815	9.5	0.849	0.151	821.4345	11	73	
		0.96	22	21.1	0.77	770	795	18.6	0.849	0.151	772.8086	11	68	
		0.98	22	21.6	0.78	780	775	11.2	0.849	0.151	781.6912	11	69	

ID	Disturbed Sample depth, m	CPT depth, m	Unit weight, γ, kN/m3	Effective vertical stress, kPa	Total cone tip resistance,	Total cone tip resistance,	AVG cone tip resistence	Pore pressure *u*, *kPa*	a factor	1-a	Total cone resistance, qt, kPa	Cone factor, Nkt	Shear strength, cu, kPa	Liquidity index, IL
1703	1.6-1.8	1.60	22	35.2	1.86	1860		107.2	0.823	0.177	1879	11	168	0.25
		1.62	22	35.6	1.94	1940	1900	115.5	0.823	0.177	1960	11	175	
		1.64	22	36.1	1.99	1990	1965	131.0	0.823	0.177	2013	11	180	
		1.66	22	36.5	1.97	1970	1980	157.3	0.823	0.177	1998	11	178	
		1.68	22	37.0	1.97	1970	1970	167.7	0.823	0.177	2000	11	178	
		1.70	22	37.4	2.09	2090	2030	194.8	0.823	0.177	2124	11	190	
		1.72	22	37.8	2.05	2050	2070	210.8	0.823	0.177	2087	11	186	
		1.74	22	38.3	2.11	2110	2080	239.2	0.823	0.177	2152	11	192	
		1.76	22	38.7	2.37	2370	2240	384.6	0.823	0.177	2438	11	218	
		1.78	22	39.2	2.37	2370	2370	317.2	0.823	0.177	2426	11	217	
		1.80	22	39.6	2.37	2370	2370	328.3	0.823	0.177	2428	11	217	

ID	Disturbed Sample depth, m	CPT depth, m	Unit weight, γ, kN/m3	Effective vertical stress, kPa	Total cone tip resistance,	Total cone tip resistance,	AVG cone tip resistence	Pore pressure *u*, *kPa*	a factor	1-a	Cone resistance, qt, kPa	Cone factor, Nkt	Shear strength, cu, kPa	Liquidity index, IL
M1701	1.1-1,.3	1.06	22	23.3	1.17	1170		41.7	0.823	0.177	1177	11	105	0.34
		1.08	22	23.8	1.10	1100	1135	63.4	0.823	0.177	1111	11	99	
		1.10	22	24.2	1.08	1080	1090	74.3	0.823	0.177	1093	11	97	
		1.12	22	24.6	1.08	1080	1080	91.1	0.823	0.177	1096	11	97	
		1.14	22	25.1	1.08	1080	1080	146.5	0.823	0.177	1106	11	98	
		1.16	22	25.5	1.06	1060	1070	171.8	0.823	0.177	1090	11	97	
		1.18	22	26.0	1.07	1070	1065	163.8	0.823	0.177	1099	11	98	
		1.20	22	26.4	1.07	1070	1070	118.8	0.823	0.177	1091	11	97	
		1.22	22	26.8	1.02	1020	1045	117.8	0.823	0.177	1041	11	92	
		1.24	22	27.3	0.83	830	925	121.5	0.823	0.177	852	11	75	
		1.26	22	27.7	0.83	830	830	142.4	0.823	0.177	855	11	75	
		1.28	22	28.2	0.83	830	830	126.4	0.823	0.177	852	11	75	
		1.30	22	28.6	0.78	780	805	91.5	0.823	0.177	796	11	70	

ID	Disturbed Sample depth, m	CPT depth, m	Unit weight, γ, kN/m3	Effective vertical stress, kPa	Total cone tip resistance, qc, MPa	Total cone tip resistance, qc, kPa	AVG cone tip resistence , qc, kPa	Pore pressure *u, kPa*	a factor	1-a	Total cone resistance, qt, kPa	Cone factor, Nkt	Shear strength, cu, kPa	Liquidity index, IL
		0.30	22	6.6	0.90	900		46.7	0.849	0.151	907	11	82	
		0.32	22	7.0	0.88	880		23.9	0.849	0.151	884	11	80	
		0.34	22	7.5	0.87	870	890	13.3	0.849	0.151	872	11	79	
		0.36	22	7.9	0.83	830	875	6.7	0.849	0.151	831	11	75	
		0.38	22	8.4	1.04	1040	850	8.6	0.849	0.151	1041	11	94	
		0.40	22	8.8	1.00	1000	935	8.0	0.849	0.151	1001	11	90	
		0.42	22	9.2	0.96	960	1020	5.7	0.849	0.151	961	11	87	
		0.44	22	9.7	0.86	860	980	15.0	0.849	0.151	862	11	78	
		0.46	22	10.1	0.89	890	910	59.2	0.849	0.151	899	11	81	
		0.48	22	10.6	0.94	940	875	72.0	0.849	0.151	951	11	85	
		0.50	22	11.0	0.96	960	915	97.3	0.849	0.151	975	11	88	
		0.52	22	11.4	1.01	1010	950	108.6	0.849	0.151	1026	11	92	
		0.54	22	11.9	1.03	1030	985	101.8	0.849	0.151	1045	11	94	
		0.56	22	12.3	1.03	1030	1020	95.9	0.849	0.151	1044	11	94	
		0.58	22	12.8	1.00	1000	1030	101.4	0.849	0.151	1015	11	91	
		0.60	22	13.2	0.99	990	1015	92.1	0.849	0.151	1004	11	90	
		0.62	22	13.6	0.98	980	995	101.6	0.849	0.151	995	11	89	
		0.64	22	14.1	0.92	920	985	112.7	0.849	0.151	937	11	84	
		0.66	22	14.5	0.92	920	950	118.4	0.849	0.151	938	11	84	
		0.68	22	15.0	0.89	890	920	116.6	0.849	0.151	908	11	81	
A1768	0.3-1.0	0.70	22	15.4	0.90	900	905	63.8	0.849	0.151	910	11	81	0.24
		0.72	22	15.8	0.83	830	895	60.0	0.849	0.151	839	11	75	
		0.74	22	16.3	0.81	810	865	56.5	0.849	0.151	819	11	73	
		0.76	22	16.7	0.93	930	820	57.0	0.849	0.151	939	11	84	
		0.78	22	17.2	1.01	1010	870	-1.6	0.849	0.151	1010	11	90	
		0.80	22	17.6	1.02	1020	970	6.5	0.849	0.151	1021	11	91	
		0.82	22	18.0	0.96	960	1015	34.5	0.849	0.151	965	11	86	
		0.84	22	18.5	0.79	790	990	114.2	0.849	0.151	807	11	72	
		0.86	22	18.9	0.79	790	875	138.3	0.849	0.151	811	11	72	
		0.88	22	19.4	0.84	840	790	120.8	0.849	0.151	858	11	76	
		0.90	22	19.8	1.00	1000	815	99.7	0.849	0.151	1015	11	90	
		0.92	22	20.2	0.93	930	920	51.4	0.849	0.151	938	11	83	
		0.94	22	20.7	0.91	910	965	37.9	0.849	0.151	916	11	81	
		0.96	22	21.1	0.90	900	920	99.7	0.849	0.151	915	11	81	
		0.98	22	21.6	0.93	930	905	113.7	0.849	0.151	947	11	84	
		1.00	22	22.0	0.90	900	915	128.4	0.849	0.151	919	11	82	
		1.02	22	22.4	0.92	917	915	106.3	0.849	0.151	933	11	83	
		1.04	22	22.9	0.91	909	909	99.2	0.849	0.151	924	11	82	
		1.06	22	23.3	0.89	893		71.2	0.849	0.151	904	11	80	
		1.08	22	23.8	0.86	860		67.2	0.849	0.151	870	11	77	

ID	Disturbed Sample depth, m	CPT depth, m	Unit weight, γ, kN/m3	Effective vertical stress, kPa	Total cone tip resistance, qc, MPa	Total cone tip resistance, qc, kPa	AVG cone tip resistence , qc, kPa	Pore pressure *u, kPa*	a factor	1-a	Total cone resistance, qt, kPa	Cone factor, Nkt	Shear strength, cu, kPa	Liquidity index, IL
		0.60	22	13.2	1.25	1250		9.8	0.823	0.177	1252	11	113	
		0.62	22	13.6	2.44	2440	1845	12.6	0.823	0.177	2442	11	221	
		0.64	22	14.1	3.13	3130	2785	-21.3	0.823	0.177	3126	11	283	
		0.66	22	14.5	2.58	2580	2855	86.0	0.823	0.177	2595	11	235	
		0.68	22	15.0	4.33	4330	3455	76.2	0.823	0.177	4343	11	394	
1704	0.6-0.8	0.70	22	15.4	2.82	2820	3575	68.1	0.823	0.177	2832	11	256	0.14
		0.72	22	15.8	2.82	2820	2820	35.8	0.823	0.177	2826	11	255	
		0.74	22	16.3	2.82	2820	2820	43.0	0.823	0.177	2828	11	256	
		0.76	22	16.7	3.14	3140	2980	28.5	0.823	0.177	3145	11	284	
		0.78	22	17.2	1.86	1860	2500	22.2	0.823	0.177	1864	11	168	
		0.80	22	17.6	1.86	1860	1860	32.5	0.823	0.177	1866	11	168	
		1.00	22	22.0	0.99	990		79.9	0.823	0.177	1004	11	89	
		1.02	22	22.4	1.10	1100	1045	87.0	0.823	0.177	1115	11	99	
		1.04	22	22.9	1.25	1250	1175	83.5	0.823	0.177	1265	11	113	
		1.06	22	23.3	0.90	900	1075	111.3	0.823	0.177	920	11	81	
		1.08	22	23.8	0.92	920	910	125.8	0.823	0.177	942	11	84	
		1.10	22	24.2	0.92	920	920	131.6	0.823	0.177	943	11	84	
		1.12	22	24.6	0.93	930	925	86.3	0.823	0.177	945	11	84	
		1.14	22	25.1	0.84	840	885	88.1	0.823	0.177	856	11	76	
1704	1.0-1.3	1.16	22	25.5	0.81	810	825	89.3	0.823	0.177	826	11	73	0.21
		1.18	22	26.0	0.81	810	810	94.2	0.823	0.177	827	11	73	
		1.20	22	26.4	0.79	790	800	102.1	0.823	0.177	808	11	71	
		1.22	22	26.8	0.75	750	770	101.9	0.823	0.177	768	11	67	
		1.24	22	27.3	0.76	760	755	101.5	0.823	0.177	778	11	68	
		1.26	22	27.7	0.89	890	825	103.0	0.823	0.177	908	11	80	
		1.28	22	28.2	0.89	890	890	109.9	0.823	0.177	909	11	80	
		1.30	22	28.6	1.07	1070	980	117.7	0.823	0.177	1091	11	97	

ID	Disturbed Sample depth, m	CPT depth, m	Unit weight, γ, kN/m3	Effective vertical stress, kPa	Total cone tip resistance,	Total cone tip resistance,	AVG cone tip resistence	Pore pressure *u*, *kPa*	a factor	1-a	Total cone resistance, qt, kPa	Cone factor, Nkt	Shear strength, cu, kPa	Liquidity index, IL
		1.60	22	35.2	1.86	1860		107.2	0.823	0.177	1879	11	168	
		1.62	22	35.6	1.94	1940	1900	115.5	0.823	0.177	1960	11	175	
		1.64	22	36.1	1.99	1990	1965	131.0	0.823	0.177	2013	11	180	
		1.66	22	36.5	1.97	1970	1980	157.3	0.823	0.177	1998	11	178	
		1.68	22	37.0	1.97	1970	1970	167.7	0.823	0.177	2000	11	178	
1703	1.6-1.8	1.70	22	37.4	2.09	2090	2030	194.8	0.823	0.177	2124	11	190	0.25
		1.72	22	37.8	2.05	2050	2070	210.8	0.823	0.177	2087	11	186	
		1.74	22	38.3	2.11	2110	2080	239.2	0.823	0.177	2152	11	192	
		1.76	22	38.7	2.37	2370	2240	384.6	0.823	0.177	2438	11	218	
		1.78	22	39.2	2.37	2370	2370	317.2	0.823	0.177	2426	11	217	
		1.80	22	39.6	2.37	2370	2370	328.3	0.823	0.177	2428	11	217	
ID	**Disturbed Sample depth, m**	**CPT depth, m**	**Unit weight, γ, kN/m3**	**Effective vertical stress, kPa**	**Total cone tip resistance,**	**Total cone tip resistance,**	**AVG cone tip resistence**	**Pore pressure *u*, *kPa***	**a factor**	**1-a**	**Cone resistance, qt, kPa**	**Cone factor, Nkt**	**Shear strength, cu, kPa**	**Liquidity index, IL**
		1.06	22	23.3	1.17	1170		41.7	0.823	0.177	1177	11	105	
		1.08	22	23.8	1.10	1100	1135	63.4	0.823	0.177	1111	11	99	
		1.10	22	24.2	1.08	1080	1090	74.3	0.823	0.177	1093	11	97	
		1.12	22	24.6	1.08	1080	1080	91.1	0.823	0.177	1096	11	97	
		1.14	22	25.1	1.08	1080	1080	146.5	0.823	0.177	1106	11	98	
		1.16	22	25.5	1.06	1060	1070	171.8	0.823	0.177	1090	11	97	
M1701	1.1-1,.3	1.18	22	26.0	1.07	1070	1065	163.8	0.823	0.177	1099	11	98	0.34
		1.20	22	26.4	1.07	1070	1070	118.8	0.823	0.177	1091	11	97	
		1.22	22	26.8	1.02	1020	1045	117.8	0.823	0.177	1041	11	92	
		1.24	22	27.3	0.83	830	925	121.5	0.823	0.177	852	11	75	
		1.26	22	27.7	0.83	830	830	142.4	0.823	0.177	855	11	75	
		1.28	22	28.2	0.83	830	830	126.4	0.823	0.177	852	11	75	
		1.30	22	28.6	0.78	780	805	91.5	0.823	0.177	796	11	70	

Appendix D. *Natural water content and liquid limit data from the Simrishamn site.*

ISO 17892-1:2014 NATURAL WATER CONTENT		Moist weight+ container,g	Dry weight+ container,g	Mass of container,mc, g	Mass of moist weight, g	Mass of dried weight,md, g	Mass of water, mw,g	Natural water content, w, %
ID	**Sample depth, m**							
17T01	2.2-2.4	50.9	45.0	1.9	49.0	43.1	5.9	13.69%
	5.7-5.9	51.7	43.5	1.7	50.0	41.8	8.2	19.62%
17T02	1.2-1.4	52.1	43.0	1.9	50.2	41.1	9.1	22.14%
	1.7-1.9	53.6	45.4	1.9	51.7	43.5	8.2	18.85%
	2.1-2.3	67.8	56.9	1.9	65.9	55.0	10.9	19.82%
	5.3-5.6	48.7	39.5	1.8	46.9	37.7	9.2	24.40%
17T04	2.1-2.3	50.7	45.4	1.8	48.9	43.6	5.3	12.16%
	3.7-3.9	37.5	30.8	1.8	35.7	29.0	6.7	23.10%

ISO/TS 17892-12:2004 LIQUID LIMIT													wL=M*w+N	
ID	**Sample depth, m**	**Measure ment**	**Cone immersion 1, mm**	**Cone immersion 2, mm**	**Cone immersion 3, mm**	**Immesrsion, AVG, mm**	**M value**	**N value**	**Mass of moist weight, g**	**Mass of dried weight, g**	**Mass of water, g**	**Water content, w, %**	**Liquid limit, wL, %**	**AVG Liquid limit, wL, %**
17T01	2.2-2.4	I	11.0	11.0	11.0	11.00	0.96	0.7	64.50	54.10	10.40	19.2%	19.15	17.45
		II	8.0	8.5	6.0	7.50	1.16	-2.7	40.10	34.60	5.50	15.9%	15.74	
	5.7-5.9	I	10.0	10.0	8.0	9.33	1.04	-0.6	45.90	34.80	11.10	31.9%	32.57	31.75
		II	12.0	10.0	10.0	10.67	0.97	0.5	40.20	30.60	9.60	31.4%	30.93	
17T02	1.2-1.4	I	8.0	10.0	10.0	9.33	1.04	-0.6	46.80	35.30	11.50	32.6%	33.28	33.28
	1.7-1.9	I	9.5	8.0	7.0	8.17	1.11	-1.8	44.40	35.10	9.30	26.5%	27.61	25.48
		II	10.0	7.0	8.0	8.33	1.10	-1.7	44.20	36.00	8.20	22.8%	23.36	
	2.1-2.3	I	9.0	7.0	7.0	7.67	1.14	-2.5	52.20	40.40	11.80	29.2%	30.80	32.13
		II	9.5	10.0	12.0	10.50	0.98	0.4	58.20	44.10	14.10	32.0%	31.73	
		III	9.0	9.0	7.0	8.33	1.10	-1.7	48.30	36.50	11.80	32.3%	33.86	
	5.3-5.6	I	12.0	12.0	10.0	11.33	0.94	0.9	52.50	35.20	17.30	49.1%	47.10	48.33
		II	10.0	8.5	8.0	8.83	1.07	-1.1	36.60	24.80	11.80	47.6%	49.81	
		III	10.0	9.0	10.0	9.67	1.01	-0.3	59.90	40.50	19.40	47.9%	48.08	
17T04	2.1-2.3	I	9.0	8.0	8.0	8.33	1.10	-1.7	45.90	38.40	7.50	19.5%	19.78	19.78
	3.7-3.9	I	8.0	8.5	10.0	8.83	1.07	-1.1	32.80	25.30	7.50	29.6%	30.62	30.28
		II	8.5	9.5	10.5	9.50	1.03	-0.4	60.30	46.70	13.60	29.1%	29.60	
		III	8	8.5	10	8.83	1.07	-1.1	32.80	25.30	7.50	29.6%	30.62	

Appendix E. *Plastic limit and summary data from the Simrishamn site*

ISO/TS 17892-12:2004 PLASTIC LIMIT		Moist weight+ container, g	Dry weight+ container, g	Mass of container, g	Mass of moist weight, g	Mass of dry weight, g	Mass of water,m w, g	Plastic limit, wp, %
ID	Sample depth, m							
17T01	2,2-2,4	15.3	13.6	2.0	13.3	11.6	1.70	14.7%
	5,7-5,9	16.5	14.3	2.0	14.5	12.3	2.20	17.9%
17T02	1,2-1,4	16.3	14.0	1.8	14.5	12.2	2.30	18.9%
	1,7-1,9	12.7	10.9	1.9	10.8	9.0	1.80	20.0%
	2,1-2,3	13.7	11.7	2.0	11.7	9.7	2.00	20.6%
	5,3-5,6	14.0	11.7	1.8	12.2	9.9	2.30	23.2%
17T04	2,1-2,3	17.5	15.6	1.9	15.6	13.7	1.90	13.9%
	3,7-3,9	14.0	11.7	1.9	12.1	9.8	2.30	23.5%

SUMMARY					Ip=wL-wp	IL=w-wp/Ip
ID	Sample depth, m	Water content,w %	Liquid limit, wL, %	Plastic limit, wp, %	Plasticity Index, Ip, %	Liquidity index, IL, %
17T01	2,2-2,4	13.69	17.45	14.66	2.79	- 0.35
	5,7-5,9	19.62	31.75	17.89	13.86	0.12
17T02	1,2-1,4	22.14	33.28	18.85	14.43	0.23
	1,7-1,9	18.85	25.48	20.00	5.48	- 0.21
	2,1-2,3	19.82	32.13	20.62	11.51	- 0.07
	5,3-5,6	24.40	48.33	23.23	25.10	0.05
17T04	2,1-2,3	12.16	19.78	13.87	5.91	- 0.29
	3,7-3,9	23.10	30.28	23.47	6.81	- 0.05

Appendix F. *CPT results from the Simrishamn site*

ID	Disturbed Sample depth, m	CPT depth, m	Unit weight, γ, kN/m3	Effective vertical stress, kPa	Total cone tip resistance, qc, MPa	Cone resistance, qc, kPa	AVG cone tip resistance, qc, kPa	Pore pressure *u, kPa*	a factor	1-a	Total cone resistance, qt, kPa	Cone factor, Nkt	Shear strength, cu, kPa	Liquidity index, IL, %
17T01	2,2-2,4	2.20	22	48.4	2.3	2250		607.7	0.846	0.154	2344	11	209	- 0.35
		2.22	22	48.8	2.4	2350		692.8	0.846	0.154	2457	11	219	
		2.24	22	49.3	4.3	4260	4582	754.5	0.846	0.154	4376	11	393	
		2.26	22	49.7	5.8	5840	5810	779.9	0.846	0.154	5960	11	537	
		2.28	22	50.2	8.2	8210	7282	186.8	0.846	0.154	8239	11	744	
		2.30	22	50.6	8.4	8390	8246	341.4	0.846	0.154	8443	11	763	
		2.32	22	51.0	9.7	9710	8988	368.2	0.846	0.154	9767	11	883	
		2.34	22	51.5	9.1	9080	8902	174.2	0.846	0.154	9107	11	823	
		2.36	22	51.9	9.6	9550	8600	78.3	0.846	0.154	9562	11	865	
		2.38	22	52.4	7.8	7780		51.0	0.846	0.154	7788	11	703	
		2.40	22	52.8	6.9	6880		92.6	0.846	0.154	6894	11	622	
ID	Disturbed Sample depth, m	CPT depth, m	Unit weight, γ, kN/m3	Effective vertical stress, kPa	Total cone tip resistance, qc, MPa	Cone resistance, qc, kPa	AVG cone tip resistance, qc, kPa	Pore pressure *u, kPa*	a factor	1-a	Total cone resistance, qt, kPa	Cone factor, Nkt	Shear strength, cu, kPa	Liquidity index, IL, %
17T01	5.7-5.9	5.70	22	125.4	2.7	2720		895.6	0.846	0.154	2858	11	248	0.12
		5.72	22	125.8	2.7	2700		882.6	0.846	0.154	2836	11	246	
		5.74	22	126.3	2.8	2750	2768	892.8	0.846	0.154	2887	11	251	
		5.76	22	126.7	2.8	2840	2768	891.2	0.846	0.154	2977	11	259	
		5.78	22	127.2	2.8	2830	2782	884.0	0.846	0.154	2966	11	258	
		5.80	22	127.6	2.7	2720	2770	869.1	0.846	0.154	2854	11	248	
		5.82	22	128.0	2.8	2770	2754	859.2	0.846	0.154	2902	11	252	
		5.84	22	128.5	2.7	2690	2750	847.9	0.846	0.154	2821	11	245	
		5.86	22	128.9	2.8	2760	2748	845.0	0.846	0.154	2890	11	251	
		5.88	22	129.4	2.8	2810		835.1	0.846	0.154	2939	11	255	
		5.90	22	129.8	2.7	2710		838.6	0.846	0.154	2839	11	246	

ID	Disturbed Sample depth, m	CPT depth, m	Unit weight, γ, kN/m3	Effective vertical stress, kPa	Cone resistance, qc, MPa	Cone resistance, qc, kPa	AVG cone tip resistance, qc, kPa	Pore pressure *u, kPa*	a factor	1-a	Total cone resistance, qt, kPa	Cone factor, Nkt	Shear strength, cu, kPa	Liquidity index, IL, %
		1.20	22	26.4	2.1	2130		96.9	0.846	0.154	2145	11	193	
		1.22	22	26.8	2.0	1990		108.3	0.846	0.154	2007	11	180	
		1.24	22	27.3	2.0	1970	2004	113.7	0.846	0.154	1988	11	178	
		1.26	22	27.7	2.0	2020	1972	125.4	0.846	0.154	2039	11	183	
		1.28	22	28.2	1.9	1910	1982	146.8	0.846	0.154	1933	11	173	
17T02	1.2-1.4	1.30	22	28.6	2.0	1970	2000	195.9	0.846	0.154	2000	11	179	0.23
		1.32	22	29.0	2.0	2040	2036	204.5	0.846	0.154	2071	11	186	
		1.34	22	29.5	2.1	2060	2112	236.1	0.846	0.154	2096	11	188	
		1.36	22	29.9	2.2	2200	2190	250.1	0.846	0.154	2239	11	201	
		1.38	22	30.4	2.3	2290		272.0	0.846	0.154	2332	11	209	
		1.40	22	30.8	2.4	2360		303.6	0.846	0.154	2407	11	216	
		1.70	22	37.4	3.8	3750		112.8	0.846	0.154	3767	11	339	
		1.72	22	37.8	3.5	3540		279.0	0.846	0.154	3583	11	322	
		1.74	22	38.3	3.5	3490	3530	404.1	0.846	0.154	3552	11	319	
		1.76	22	38.7	3.5	3530	3432	449.2	0.846	0.154	3599	11	324	
		1.78	22	39.2	3.3	3340	3362	477.1	0.846	0.154	3413	11	307	
17T02	1.7-1.9	1.80	22	39.6	3.3	3260	3300	601.9	0.846	0.154	3353	11	301	0.21
		1.82	22	40.0	3.2	3190	3216	901.1	0.846	0.154	3329	11	299	
		1.84	22	40.5	3.2	3180	3148	574.6	0.846	0.154	3268	11	293	
		1.86	22	40.9	3.1	3110	3078	553.1	0.846	0.154	3195	11	287	
		1.88	22	41.4	3.0	3000		542.2	0.846	0.154	3083	11	277	
		1.90	22	41.8	2.9	2910		549.5	0.846	0.154	2995	11	268	

ID	Disturbed Sample depth, m	CPT depth, m	Unit weight, γ, kN/m3	Effective vertical stress, kPa	Cone resistance, qc, MPa	Cone resistance, qc, kPa	AVG cone tip resistance, qc, kPa	Pore pressure *u, kPa*	a factor	1-a	Total cone resistance, qt, kPa	Cone factor, Nkt	Shear strength, cu, kPa	Liquidity index, IL, %
		2.16	22	47.5	2.8	2830		422.0	0.846	0.154	2895	11	259	
		2.18	22	48.0	2.8	2840		406.5	0.846	0.154	2903	11	260	
		2.20	22	48.4	2.7	2700	2736	341.8	0.846	0.154	2753	11	246	
17T02	2.16-2.3	2.22	22	48.8	2.7	2650	2786	361.7	0.846	0.154	2706	11	242	0.07
		2.24	22	49.3	2.7	2660	2926	450.2	0.846	0.154	2729	11	244	
		2.26	22	49.7	3.1	3080	3022	591.8	0.846	0.154	3171	11	284	
		2.28	22	50.2	3.5	3540		531.0	0.846	0.154	3622	11	325	
		2.30	22	50.6	3.2	3180		450.6	0.846	0.154	3249	11	291	

ID	Disturbed Sample depth, m	CPT depth, m	Unit weight, γ, kN/m3	Effective vertical stress, kPa	Cone resistance, qc, MPa	Cone resistance, qc, kPa	AVG cone tip resistance, qc, kPa	Pore pressure *u, kPa*	a factor	1-a	Total cone resistance, qt, kPa	Cone factor, Nkt	Shear strength, cu, kPa	Liquidity index, IL, %
		5.30	22	116.6	2.1	2060		212.2	0.846	0.154	2093	11	180	
		5.32	22	117.0	2.2	2210		214.3	0.846	0.154	2243	11	193	
		5.34	22	117.5	2.6	2560	2446	210.9	0.846	0.154	2592	11	225	
		5.36	22	117.9	2.7	2670	2584	221.8	0.846	0.154	2704	11	235	
		5.38	22	118.4	2.7	2730	2682	212.4	0.846	0.154	2763	11	240	
		5.40	22	118.8	2.8	2750	2682	208.8	0.846	0.154	2782	11	242	
		5.42	22	119.2	2.7	2700	2666	205.6	0.846	0.154	2732	11	237	
17T02	5.3-5.6	5.44	22	119.7	2.6	2560	2620	206.1	0.846	0.154	2592	11	225	0.05
		5.46	22	120.1	2.6	2590	2546	210.8	0.846	0.154	2622	11	227	
		5.48	22	120.6	2.5	2500	2482	204.5	0.846	0.154	2531	11	219	
		5.50	22	121.0	2.4	2380	2442	209.9	0.846	0.154	2412	11	208	
		5.52	22	121.4	2.4	2380	2360	208.9	0.846	0.154	2412	11	208	
		5.54	22	121.9	2.4	2360	2326	208.5	0.846	0.154	2392	11	206	
		5.56	22	122.3	2.2	2180	2316	208.1	0.846	0.154	2212	11	190	
		5.58	22	122.8	2.3	2330		221.0	0.846	0.154	2364	11	204	
		5.60	22	123.2	2.3	2330		221.0	0.846	0.154	2364	11	204	

ID	Disturbed Sample depth, m	CPT depth, m	Unit weight, γ, kN/m3	Effective vertical stress, kPa	Cone resistance, qc, MPa	Cone resistance, qc, kPa	AVG cone tip resistance, qc, kPa	Pore pressure *u, kPa*	a factor	1-a	Total cone resistance, qt, kPa	Cone factor, Nkt	Shear strength, cu, kPa	Liquidity index, IL, %
		2.10	22	46.20	6.0	6030		385.8	0.846	0.154	6089.4	11	549	
		2.12	22	46.64	4.4	4430		339.2	0.846	0.154	4482.2	11	403	
		2.14	22	47.08	4.0	4010	4570	317.0	0.846	0.154	4058.8	11	365	
		2.16	22	47.52	4.1	4050	4334	415.2	0.846	0.154	4113.9	11	370	
		2.18	22	47.96	4.3	4330	4420	444.0	0.846	0.154	4398.4	11	395	
17T04	2.1-2.3	2.20	22	48.40	4.9	4850	4540	527.4	0.846	0.154	4931.2	11	444	0.29
		2.22	22	48.84	4.9	4860	4524	488.3	0.846	0.154	4935.2	11	444	
		2.24	22	49.28	4.6	4610	4340	314.6	0.846	0.154	4658.4	11	419	
		2.26	22	49.72	4.0	3970	3926	163.4	0.846	0.154	3995.2	11	359	
		2.28	22	50.16	3.4	3410		172.9	0.846	0.154	3436.6	11	308	
		2.30	22	50.60	2.8	2780		203.4	0.846	0.154	2811.3	11	251	
		3.70	22	81.4	4.6	4580		981.9	0.846	0.154	4731.2	11	423	
		3.72	22	81.8	4.6	4580		981.9	0.846	0.154	4731.2	11	423	
		3.74	22	82.3	5.0	4950	4472	715.1	0.846	0.154	5060.1	11	453	
		3.76	22	82.7	4.6	4630	4248	649.3	0.846	0.154	4730.0	11	422	
		3.78	22	83.2	3.6	3620	4026	405.4	0.846	0.154	3682.4	11	327	
17T04	3.7-3.9	3.80	22	83.6	3.5	3460	3726	449.3	0.846	0.154	3529.2	11	313	0.05
		3.82	22	84.0	3.5	3470	3458	495.6	0.846	0.154	3546.3	11	315	
		3.84	22	84.5	3.5	3450	3402	519.1	0.846	0.154	3529.9	11	313	
		3.86	22	84.9	3.3	3290	3380	600.3	0.846	0.154	3382.4	11	300	
		3.88	22	85.4	3.3	3340		550.2	0.846	0.154	3424.7	11	304	
		3.90	22	85.8	3.4	3350		555.8	0.846	0.154	3435.6	11	305	

Tidigare skrifter i serien ”Examensarbeten i Geologi vid Lunds universitet”:

493. Kristensson, Johan, 2016: Formation evaluation of the Jurassic Stø and Nordmela formations in exploration well 7220/8-1, Barents Sea, Norway. (45 hp)
494. Larsson, Måns, 2016: TEM investigation on Challapampa aquifer, Oruro Bolivia. (45 hp)
495. Nylén, Fredrik, 2017: Utvärdering av borrhålskartering avseende kalksten för industriella ändamål, File Hajdarbrottet, Slite, Gotland. (45 hp)
496. Mårdh, Joakim, 2017: A geophysical survey (TEM; ERT) of the Punata alluvial fan, Bolivia. (45 hp)
497. Skoglund, Wiktor, 2017: Provenansstudie av detriala zirkoner från ett guldförande alluvium vid Ravlunda skjutfält, Skåne. (15 hp)
498. Bergcrantz, Jacob, 2017: Ett fönster till Kattegatts förflutna genom analys av bottenlevande foraminiferer. (15 hp)
499. O'Hare, Paschal, 2017: Multiradionuclide evidence for an extreme solar proton event around 2610 BP. (45 hp)
500. Goodship, Alastair, 2017: Dynamics of a retreating ice sheet: A LiDAR study in Värmland, SW Sweden. (45 hp)
501. Lindvall, Alma, 2017: Hur snabbt påverkas och nollställs luminiscenssignaler under naturliga ljusförhållanden? (15 hp)
502. Sköld, Carl, 2017: Analys av stabila isotoper med beräkning av blandningsförhållande i ett grundvattenmagasin i Älvkarleby-Skutskär. (15 hp)
503. Sällström, Oskar, 2017: Tolkning av geofysiska mätningar i hammarborrhål på södra Gotland. (15 hp)
504. Ahrenstedt, Viktor, 2017: Depositional history of the Neoproterozoic Visingsö Group, south-central Sweden. (15 hp)
505. Schou, Dagmar Juul, 2017: Geometry and faulting history of the Long Spur fault zone, Castle Hill Basin, New Zealand. (15 hp)
506. Andersson, Setina, 2017: Skalbärande marina organismer och petrografi av tidigcampanska sediment i Kristianstadsbassängen – implikationer på paleomiljö. (15 hp)
507. Kempengren, Henrik, 2017: Föroreningsspridning från kustnära deponi: Applicering av Landsim 2.5 för modellering av lakvattentransport till Östersjön. (15 hp)
508. Ekborg, Charlotte, 2017: En studie på samband mellan jordmekaniska egenskaper och hydrodynamiska processer när erosion påverkar släntstabiliteten vid ökad nederbörd. (15 hp)
509. Silvén, Björn, 2017: LiDARstudie av glaciala landformer sydväst om Söderåsen, Skåne, Sverige. (15 hp)
510. Rönning, Lydia, 2017: Ceratopsida dinosauriers migrationsmönster under krittiden baserat på paleobiogeografi och fylogeni. (15 hp)
511. Engleson, Kristina, 2017: Miljökonsekvensbeskrivning Revinge brunnsfält. (15 hp)
512. Ingered, Mimmi, 2017: U-Pb datering av zirkon från migmatitisk gnejs i Delsjöområdet, Idefjordenterrängen. (15 hp)
513. Kervall, Hanna, 2017: EGS - framtidens geotermiska system. (15 hp)
514. Walheim, Karin, 2017: Kvartsmineralogins betydelse för en lyckad luminiscensdatering. (15 hp)
515. Aldenius, Erik, 2017: Lunds Geotermisystem, en utvärdering av 30 års drift. (15 hp)
516. Aulin, Linda, 2017: Constraining the duration of eruptions of the Rangitoto volcano, New Zealand, using paleomagnetism. (15 hp)
517. Hydén, Christina Engberg, 2017: Drumlinerna i Löberöd - Spår efter flera isrörelseriktningar i mellersta Skåne. (15 hp)
518. Svantesson, Fredrik, 2017: Metodik för kartläggning och klassificering av erosion och släntstabilitet i vattendrag. (45 hp)
519. Stjern, Rebecka, 2017: Hur påverkas luminiscenssignaler från kvarts under laboratorieförhållanden? (15 hp)
520. Karlstedt, Filippa, 2017: P-T estimation of the metamorphism of gabbro to garnet amphibolite at Herrestad, Eastern Segment of the Sveconorwegian orogen. (45 hp)
521. Önnervik, Oscar, 2017: Ooider som naturliga arkiv för förändringar i havens geokemi och jordens klimat. (15 hp)
522. Nilsson, Hanna, 2017: Kartläggning av sand och naturgrus med hjälp av resistivitetsmätning på Själland, Danmark. (15 hp)
523. Christensson, Lisa, 2017: Geofysisk undersökning av grundvattenskydd för planerad reservvattentäkt i Mjölkalånga, Hässleholms kommun. (15 hp)
524. Stamsnijder, Joaen, 2017: New geochronological constraints on the Klipriviersberg Group: defining a new Neoarchean large igneous province on the Kaapvaal Craton, South Africa. (45 hp)
525. Becker Jensen, Amanda, 2017: Den eocena Furformationen i Danmark: exceptionella bevaringstillstånd har bidragit till att djurs mjukdelar fossiliserats.(15 hp)
526. Radomski, Jan, 2018: Carbonate sedimen-

tology and carbon isotope stratigraphy of the Tallbacken-1 core, early Wenlock Slite Group, Gotland, Sweden. (45 hp)

527. Pettersson, Johan, 2018: Ultrastructure and biomolecular composition of sea turtle epidermal remains from the Campanian (Upper Cretaceous) North Sulphur River of Texas. (45 hp)

528. Jansson, Robin, 2018: Multidisciplinary perspective on a natural attenuation zone in a PCE contaminated aquifer. (45 hp)

529. Larsson, Alfred, 2018: Rb-Sr sphalerite data and implications for the source and timing of Pb-Zn deposits at the Caledonian margin in Sweden. (45 hp)

530. Balija, Fisnik, 2018: Stratigraphy and pyrite geochemistry of the Lower–Upper Ordovician in the Lerhamn and Fågelsång -3 drill cores, Scania, Sweden. (45 hp)

531. Höglund, Nikolas, 2018: Groundwater chemistry evaluation and a GIS-based approach for determining groundwater potential in Mörbylånga, Sweden. (45 hp)

532. Haag, Vendela, 2018: Studie av mikrostrukturer i karbonatslagkäglor från nedslagsstrukturen Charlevoix, Kanada. (15 hp)

533. Hebrard, Benoit, 2018: Antropocen – vad, när och hur? (15 hp)

534. Jancsak, Nathalie, 2018: Åtgärder mot kusterosion i Skåne, samt en fallstudie av erosionsskydden i Löderup, Ystad kommun. (15 hp)

535. Zachén, Gabriel, 2018: Mesosideriter – redogörelse av bildningsprocesser samt SEM-analys av Vaca Muertameteoriten. (15 hp)

536. Fägersten, Andreas, 2018: Lateral variability in the quantification of calcareous nannofossils in the Upper Triassic, Austria. (15 hp)

537. Hjertman, Anna, 2018: Förutsättningar för djupinfiltration av ytvatten från Ivösjön till Kristianstadbassängen. (15 hp)

538. Lagerstam, Clarence, 2018: Varför svalde svanödlor (Reptilia, Plesiosauria) stenar? (15 hp)

539. Pilser, Hannes, 2018: Mg/Ca i bottenlevande foraminiferer, särskilt med avseende på temperaturer nära 0°C. (15 hp)

540. Christiansen, Emma, 2018: Mikroplast på och i havsbotten - Utbredningen av mikroplaster i marina bottensediment och dess påverkan på marina miljöer. (15 hp)

541. Staahlnacke, Simon, 2018: En sammanställning av norra Skånes prekambriska berggrund. (15 hp)

542. Martell, Josefin, 2018: Shock metamorphic features in zircon grains from the Mien impact structure - clues to conditions during impact. (45 hp)

543. Chitindingu, Tawonga, 2018: Petrological characterization of the Cambrian sandstone reservoirs in the Baltic Basin, Sweden. (45 hp)

544. Chonewicz, Julia, 2018: Dimensionerande vattenförbrukning av grundvatten samt alternativa vattenkvaliteter. (15 hp)

545. Adeen, Lina, 2018: Hur lämpliga är de geofysiska metoderna resistivitet och IP för kartläggning av PFOS? (15 hp)

546. Nilsson Brunlid, Anette, 2018: Impact of southern Baltic sea-level changes on landscape development in the Verkeån River valley at Haväng, southern Sweden, during the early and mid Holocene. (45 hp)

547. Perälä, Jesper, 2018: Dynamic Recrystallization in the Sveconorwegian Frontal Wedge, Småland, southern Sweden. (45 hp)

548. Artursson, Christopher, 2018: Stratigraphy, sedimentology and geophysical assessment of the early Silurian Halla and Klinteberg formations, Altajme core, Gotland, Sweden. (45 hp)

549. Kempengren, Henrik, 2018: Att välja den mest hållbara efterbehandlingsmetoden vid sanering: Applicering av beslutsstödsverktyget SAMLA. (45 hp)

550. Andreasson, Dagnija, 2018: Assessment of using liquidity index for the approximation of undrained shear strength of clay tills in Scania. (45 hp)

LUNDS UNIVERSITET

Geologiska institutionen
Lunds universitet
Sölvegatan 12, 223 62 Lund